

https://dspace.org/

Microwave-assisted synthesis of -CD polymers incorporating N-doped carbon nanotubes and silver nanoparticles for water purification

Masinga, Sello Petros

2013-07-29
http://hdl.handle.net/10539/12919

Downloaded from a DSpace repository. https://dspace.org/

Microwave-assisted Synthesis of β-CD Polymers Incorporating N-doped Carbon Nanotubes and Silver Nanoparticles for Water Purification

By

Sello Petros Masinga

Student Number: 0706373f

A dissertation submitted to the Faculty of Science, University of the Witwatersrand, Johannesburg, in fulfilment of a Master of Science degree in Chemistry.

Supervisor:	Dr S.D. Mhlanga
Co-supervisors:	Prof. B.B. Mamba
	Dr E.N. Nxumalo

University of the Witwatersrand, May 2013

DECLARATION

I, Sello Masinga, hereby declare that the dissertation which I herewith submit for the research qualification

MASTERS DEGREE IN CHEMISTRY

to the University of the Witwatersrand, Department of Chemistry is, apart from the recognised assistance of my supervisor, my own work and has not been previously been submitted by me to another institution to obtain a degree.

DEDICATION

I dedicate this work to my parents, my beautiful siblings and my niece for their support and inspiration they invoked in me. To my heavenly Father, God almighty, the third hand in this work, I am eternally grateful for His enduring love that He lavishly poured upon me and the grace that you used to spoil me. No words can truly express and communicate my love for Him.

ACKNOWLEDGEMENTS

I would like to acknowledge a handful of people and organisations that God has placed within my reach to successfully complete the project:

- Dr Sabelo Mhlanga (supervisor and mentor), Dr Edward Nxumalo and Prof. Bhekie Mamba (co-supervisors).
- Prof Neil Coville (research advisor).
- Miss Zikhona Tetana and Miss Manoko Maubane who got me started with preliminaries in the lab.
- The CATOMMAT group for its assistance with regards to presentation skills and criticism during my seminar presentations.
- Dr Kulsum Kondiah for her assistance in antibacterial studies.
- The Analytical Chemistry research group for provision of SPE equipment.

Institutions and companies:

- University of the Witwatersrand (School of Chemistry and Wits Medical School).
- Mintek.

Financial support

- DST/Mintek Nanotechnology Innovation Centre (NIC) for my bursary.
- BRADLOW Scholarship from financial aid office.

ABSTRACT

The pollution of water sources by chemical and biological species has created a serious water crisis all over the world. Such pollution has placed severe strains on the limited water sources resulting in the spread of waterborne diseases, which continue to be the leading causes of deaths in developing countries. Pollution by organic species still poses a serious health and environmental problem. Attempts to mitigate this problem are on-going and a number of methods are employed currently. Activated carbon and reverse osmosis are some of the current techniques that are used for the removal of organics in water. However, these techniques are limited in the removal of pollutants at lower concentrations (ng/L). Recent studies demonstrated the efficient removal of organics by nanoporous cyclodextrin (CD) polymers, a class of nanomaterials with great potential in absorbing organic pollutants from water.

This project reports on the synthesis of β-cyclodextrin (β-CD) based polymer nanocomposite materials (nanocomposites) that have been blended with nitrogen-doped carbon nanotubes (N-CNTs) and silver (Ag) nanoparticles for water treatment. Prior to this study, the synthesis of these nanocomposites has been based on a conventional method that involves heating the reactants in a round bottom flask for 16 – 24 h. In this study a new method that is efficient, greener and time saving is reported. This facile method involved synthesizing the polymer nanocomposites under microwave irradiation wherein complete synthesis of the polymer nanocomposites was achieved in 10 min.

N-CNTs were first synthesized via modified chemical vapour deposition method (CVD) using a 10wt% Fe-Co/$CaCO_3$ catalyst. The N-CNTs were found to contain ~ 2% nitrogen by CN and XPS analysis. The N-CNTs were of high purity and were oxidized with acid functional groups (-COOH, -C=O, -OH) using nitric acid under reflux. Zeta potential studies indicated that the quantity of acid functional groups increased with increase in acid treatment time. The functionalised N-CNTs (*f*N-CNTs) were then decorated with Ag nanoparticles using microwave irradiation and further polymerized with β-CD using hexamethylene diisocyanate (HMDI) as the linker in an industrial microwave under an inert gas atmosphere of N_2.

Two types of polymer nanocomposites were synthesized namely, N-CNTs/β-CD and Ag/N-CNTs/β-CD. Different synthesis parameters such as microwave power and time were varied during the synthesis of these composites to study their effect on the result materials. Different level of power, 400 W, 600 W and 800 W were tested and surface area and morphology data indicated that all these powers can be used in synthesising the polymer composites. The optimum power used was 600 W, which gave highly porous, less densely packed morphology and a higher surface area of the polymers. The synthesis time was varied for 10 min, 15 min and 30 min. An irradiation time of 10 min was found to be sufficient for the synthesis of the nanocomposites. The polymers showed an efficient removal of *p*-nitrophenol, bisphenol A and trichloroethylene (TCE) from spiked water as confirmed by UV-Vis spectroscopy and GC/MS analysis.

TABLE OF CONTENTS

Declaration……......i

Dedication…….. ii

Acknowledgements….. iii

Abstract…….....iv

Table of contents vi

List of abbreviations x

List of figures…….....xii

List of tables……..xiv

Publications and presentations at conferences.....xv

CHAPTER 1: INTRODUCTION

1.1 Background.....1

1.2 Justification.....3

1.3 Aim of the research study 4

1.4 Outline of dissertation.....5

CHAPTER 2: LITERATURE REVIEW

2.1 Global water problems.....6

2.1.1 Pollution by organic compounds 6

2.1.1.1 Natural organic matter (NOM) 6

2.1.1.2 Phenols.....7

2.1.1.3 Water disinfection by-products.....10

2.1.2 Pollution by inorganic compounds 11
2.1.2.1 Heavy metals 11
2.1.2.2 Anions 12
2.1.3 Pollution by microorganisms 12
2.1.3.1 Cryptosporidium parvum 12
2.1.3.2 Escherichia coli 13
2.1.3.3 Shigella spp 13
2.2 Water treatment technologies 14
2.2.1 Conventional technologies 14
2.2.1.1 Chlorination 14
2.2.1.2 Ozonation 14
2.2.1.3 Ultraviolet radiation 15
2.2.1.4 Granular activated carbon 15
2.2.2 Technologies based on nanostructured materials 17
2.2.2.1 Membrane technologies 17
2.2.2.2 Noble metal nanoparticles 18
2.2.2.3 Polymer nanocomposite materials 20
2.3 Adsorption capacities of various media for removal of phenolics 25
2.4 Carbon nanotubes and doped carbon nanotubes 26
2.5 Green chemistry 29
2.6 Microwave synthesis 30

CHAPTER 3: EXPERIMENTAL

3.1 Synthesis of catalysts 33
3.2 Synthesis of N-CNTs 33

3.3 Conventional synthesis of N-CNTs/β-CD polymer composite 34
3.4 Microwave-assisted synthesis of N-CNT/β-CD polymer composite 34
3.5 Removal of *p*-nitrophenol 35
3.6 Removal of trichloroethylene (TCE) and bisphenol A 35
3.7 Microwave synthesise of Ag/N-CNTs 35
3.8 Microwave synthesis of Ag/N-CNTs/β-CD 36
3.9 Antibacterial testing 36

CHAPTER 4: CHARACTERIZATION AND APPLICATION OF *f*N-CNTs/β-CD POLYMER NANOCOMPOSITES

4.1 Characterization of N-CNTs 37
4.1.1 TEM…… 37
4.1.2 CN and XPS analysis 38
4.1.3 TG analysis (TGA) 40
4.1.4 FT-IR analysis and Zeta potential analysis 41
4.1.5 Surface area analysis of the N-CNTs 43
4.2 Characterization of fN-CNTs/β-CD nanocomposite materials 44
4.2.1 FT-IR analysis 44
4.2.2 TG analysis (TGA) 45
4.2.3 Structural morphology of the polymer nanocomposites 47
4.2.4 Surface area of fN-CNTs/β-CD polymer nanocomposites 49
4.3 UV-VIS analysis for the removal p-nitrophenol 50
5.1 Characterisation of Ag/fN-CNTs 53
5.1.1 TEM and EDS analysis 53
5.1.2 TG analysis of Ag/fN-CNTs 55
5.2 Characterization of Ag/fN-CNTs/ β-CD nanocomposites 56

5.2.1 FT-IR analysis....56
5.2.2 TG analysis....56
5.2.3 Structural morphology and EDS analysis of 20 wt.% Ag/N-CNTs/β-CD polymer nanocomposites....57
5.2.4 Surface area of 20wt%Agf/N-CNTs/β-CD polymer nanocomposite....59
5.3 Removal of bisphenol A, trichloroethylene and p-nitrophenol by Ag/fN-CNTs/ β-CD polymer nanocomposites....59
5.4 Antibacterial studies....60
5.4.1 Bacterial activity of 20 wt.% Ag/fN-CNTs....60
5.4.2 Bacterial activity of 20wt%Ag/fN-CNTs/β-CD polymer nanocomposite....61

CHAPTER 6: CONCLUSIONS AND RECOMMENDATIONS

6.1 Conclusions....63
6.2 Recommendation for future work....64

REFERENCES....65

LIST OF ABBREVIATIONS

α-CD	Alpha Cyclodextrin
β-CD	Beta Cyclodextrin
BET	Branauer Emmett and Teller
CN	Carbon Nitrogen analysis
CVD	Chemical Vapour Deposition
CGTase	Cycloglycosyl Transferase
DNA	Deoxyribonucleic acid
DOM	Dissolved Organic Matter
DMF	Dimethyl formamide
DBPs	Disinfection By-products
EDS	Energy Dispersive Spectroscopy
FT-IR	Fourier Transform Infrared
FO	Forward Osmosis
GC-MS	Gas Chromatograph/Mass Spectrometry
GAC	Granular Activated Carbon
γ-CD	Gamma Cyclodextrin
HMDI	Hexamethylene Diisocynate
LED	Light Emitting Diode
MWNT(s)	Multi Walled Carbon Nanotube(s)
NOM	Natural Organic Matter
NDMA	Nitrodiniethylamine
N-CNTs	Nitrogen-doped Carbon Nanotubes
NP	Nanoparticles
ng/L	nanograms per litre
PNP	Para Nitrophenol
PCB	Polychlorinated Bisphenol
PZC	Point of Zero Charge
RO	Reverse Osmosis
SEM	Scanning Electron Microscopy
SWNT(s)	Single Walled Carbon Nanotube(s)
SPE	Solid Phase Extraction
TEM	Transmission Electron Microscopy

TGA	Thermal Gravimetric Analysis
TDI	2, 4 Toulene Diisocynate
TCE	Trichloroethylene
THM	Trihalomethanes
UV-Vis	Ultraviolet- Visible
WHO	World Health Organisation
XPS	X-ray Photoelectron Spectroscopy
ZVI	Zero Valent Iron

LIST OF FIGURES

Figure	***Description***	***Page***
Fig. 1:	Examples of NOM found in water: a) humic acid and b) glucose.	**7**
Fig. 2:	The structure of *p*-nitrophenol.	**8**
Fig. 3:	Structure of bisphenol A.	**9**
Fig. 4:	The structure of trichloroethylene.	**10**
Fig. 5:	The structures of different haloacetic acids found in water.	**11**
Fig. 6:	Various mechanisms of antimicrobial activities exerted by nanomaterials.	**20**
Fig. 7:	Structures of the different CDs showing different numbers of glucopyranose units forming the cyclic oligomer.	**22**
Fig. 8:	Schematic representation of β-CD indicating the different hydroxyl group in the structure.	**23**
Fig. 9:	Schematic representation of CD-guest complex formation in water.	**24**
Fig. 10:	Synthetic pathway for cyclodextrin polyurethanes.	**25**
Fig. 11:	Structures of single and multi-walled CNTs.	**27**
Fig. 12:	Different ways to modify nanotube electronic properties.	**29**
Fig. 13:	Chemical vapour deposition set-up for the synthesis of N-CNTs.	**34**
Fig. 14:	TEM images of the synthesized N-CNTs before (a) and after purification (b).	**37**
Fig. 15:	Outer diameter distribution of the purified N-CNTs.	**38**
Fig. 16:	Types of nitrogen moieties that can be incorporated into graphitic carbon: (A) oxidized pyridinic, (B) pyridinic, (C) pyrrolic, (D) quaternary.	**39**
Fig. 17:	XPS spectrum showing a deconvoluted N 1s spectrum of the functionalized N-CNTs.	**38**
Fig. 18:	TGA profiles of the as-synthesized N-CNTs and *f*N-CNTs refluxed in HNO_3 at different times.	**39**
Fig. 19:	FT-IR spectra of the as-synthesized and *f*N-CNTs refluxed in HNO_3 at different times.	**42**
Fig. 20:	Zeta potential measurements of the as-synthesized and *f* N-CNTs as a function of pH.	**43**
Fig. 21:	FTIR spectra of the polymer nanocomposites showing the absence of the isocyanate peak. The absence of the peak suggests complete polymerization.	**44**

Fig. 22: FTIR spectra of the polymer nanocomposites synthesized at different microwave irradiation powers, 400 W, 600 W and 800 W for 10 min. **45**

Fig. 23: Derivative weight % profiles for β-CD and *f*N-CNTs/β-CD synthesized via the conventional and microwave-induced methods. **46**

Fig. 24: Derivative weight % profiles for β-CD and *f*N-CNTs/β-CD synthesized via the microwave-induced method at different irradiation powers. **47**

Fig. 25: SEM images of the *f*N-CNTs/β-CD polymer nanocomposites synthesized by the conventional method (a) and microwave method (b). **48**

Fig. 26: SEM images of the *f*N-CNTs/β-CD polymer nanocomposites synthesized by microwave-induced method at different irradiation powers 400 W (a), 600 W (b), 800 W (c). **48**

Fig. 27: UV-Vis Absorbance spectra for *f*N-CNTs/β-CD polymer composite synthesized *via* the conventional and microwave methods. **51**

Fig. 28: Colour changes of spiked water samples before (left) and after (right) percolation through polymer matrix. **52**

Fig. 29: (a) A TEM and high magnification image (inset) of Ag/N-CNTs prepared under microwave irradiation; (b) a TEM and high magnification image (inset) of Ag/N-CNTs prepared using the wet impregnation method. The dark sports are the Ag NPs. **53**

Fig. 30: Diameter distribution of the Ag nanoparticles. **54**

Fig. 31: EDS confirming the presence of Ag nanoparticles in 20wt%Ag/N-CNTs. **54**

Fig. 32: Weight loss profile for *f*N-CNTs and Ag-NCNTs. **55**

Fig. 33: FTIR spectra of the confirming the successful synthesis of 20wt%Ag/NCNTs/β-CD polymer nanocomposite. **56**

Fig. 34: Derivative weight loss profile for native β-CD, N-CNTs/β-CD and 20wt%Ag/N-CNTs/β-CD polymer nanocomposites. **57**

Fig. 35: SEM micrograph of 20wt%Ag/N-CNTs/β-CD polymer nanocomposites. **58**

Fig. 36: EDS confirming the presence of Ag nanoparticles in 20wt%Ag/N-CNTs/β-CD polymer nanocomposite. **59**

Fig. 37: Images showing the zone of inhibition at time 0 (a) and after 24 h (b). **61**

LIST OF TABLES

Tables ***Description*** ***Page***

Table 1: Advantages and disadvantages of the various conventional technologies in water treatment **16**

Table 2: Characteristics of α, β, γ cyclodextrins. **22**

Table 3: Adsorption capacities of various adsorption media for removal of *p*-nitrophenol in water **25**

Table 4: BET surface areas of the as-synthesized and *f*N-CNTs used to prepare polymer composites with β-CDs. **43**

Table 5: Surface area of conventional and microwave synthesized *f*N-CNTs/β-CD polymer nanocomposites. **49**

Table 6: Surface area of *f*N-CNTs/β-CD polymer nanocomposites synthesized at different synthesis times. **50**

Table 7: Amounts (percentage) of organic pollutant removed after passing water samples containing 20 µg/L of pollutant through the Ag/N-CNT/β-CD polymer nanocomposites. **60**

Table 8: *E.coli* cell counts after 3 and 24 h of exposure to 20wt%Ag/N-CNTs/β-CD polymer nanocomposite. **62**

PUBLICATIONS AND PRESENTATION AT CONFERENCES

Publications

- S.D. Mhlanga, S.P. Masinga, M.F. Bambo, B.B. Mamba, E.N. Nxumalo, A Facile Procedure to Synthesize a Three-Component β-cyclodextrin Polyurethane Nanocomposite Matrix Containing Ag Decorated N-CNTs for Water Treatment, *Nanosci. Nanotechnol. Lett.*, Vol. 5, 2013, article in press.

- S.P. Masinga, E.N. Nxumalo, B.B. Mamba, S.D. Mhlanga, Microwave-induced Synthesis of Ag/N-CNT β-CD Nanoporous Polyurethane Nanocomposites for Water Purification, submitted, *Environmental Science and Pollution Research*, 2012.

Conference and Workshops

- DST/Mintek Nanotechnology Innovative Centre (NIC) workshops in 2011 (Poster, Mintek, Randburg) and 2012 (Oral, Medical Research Council, Cape Town). Obtained best poster presentation in 2011.

- NanoAfrica 2012 - the 4th International Conference on Nanoscience and Nanotechnology, University of the Free State, Bloemfontein, 1 – 4 April 2012, Oral.

- The 13th Waternet/WARFSA/GWP-SA Symposium, Birchwood Hotel, Boksburg, November 2012, Poster.

- Two oral presentations were given at the CATOMAT group seminars in 2011 and 2012.

CHAPTER 1: INTRODUCTION

1.1 Background

Water is a scarce and precious natural resource that is vital for the existence and serenity of life. It constitutes a critical 70% of the human body weight, and can be regarded as the most valuable resource [1]. However, the pollution of water sources by chemical and biological species has created a serious water crisis all over the world. Such pollution has placed severe strains on the limited water sources resulting in the spread of waterborne diseases which continue to be the leading causes of deaths in developing countries. As consequence the water industry has shifted its focus to reclamation, reuse and recycling of raw water, wastewater and seawater desalination [2].

A number of methods have been developed an attempt to meet drinking water quality standards. Current methods rely on chemical oxidants such as free chlorine, chloramines, and ozone which are reported to effectively destroy bacteria and viruses in water [2]. However, these chemical disinfection methods have a number of drawbacks, e.g. they produce harmful disinfection by-products that are formed when chlorine reacts with water to form hypochlorous acid which in turn reacts with natural organic matter (NOM) such as humic acid and fulvic acid to form the disinfection by-products (DBPs) such as halo-carbons (trihalomethanes, polychlorinated biphenyls etc.). DBPs are known to be carcinogens and endocrine disruptors [2-4]. They are also known to be persistent in water. Carcinogenic nitrosodiniethylamine (NDMA) and bromates are also produced when monochloramine or chlorine reacts with ammonia and organic amines, and when ozone reacts with bromides respectively [2]. Clearly while these methods are useful, they also create other problems. As such, innovative approaches that will not only attempt to meet the water standards set by the World Health Organisation (WHO) [5] but also avoid unintended adverse health effects are required. It is under this context that a great deal of research is performed to produce nanotechnologies based on nanomaterials to circumvent the challenges relating to water quality.

A number of nanomaterials have been synthesized for water treatment purposes such as nanoclays, for removal of metal cations [6] and organics [1], alumina nanoparticles for heavy metal removal [1, 7] and iron-based nanomaterials such as zero valent iron (ZVI) for removal of halogenated organics, arsenic, heavy metals, nitrates etc. [1, 8] and Fe_3O_4 nanoparticles for removal of arsenic from water [1, 9]. Amongst these materials are the advanced nanocomposite materials of cyclodextrin (CD) polymers incorporating carbon nanotubes (CNTs) [3, 4, 10-13]. CDs are starch based cyclic oligomers formed by the 1, 4 linkages of glucose units [14, 15]. They are found in nature through enzymatic degradation of starch molecules by amylase bacteria and cycloglycosyl transferase (CGTase). There are three classes of CDs, namely α-CD (6), β-CD (7) and γ-CD (8) which differs in their number of glucose molecules in the cyclic chain. β-CD is the most widely used because it is the most accessible, the cheapest and exhibits the highest reactivity [15].

β-CD based insoluble polymers have demonstrated an ability to remove organic pollutants in water in concentration levels as low as ng L^{-1} [3, 15]. However through a series of recycling procedures, the structural integrity of the polymer becomes compromised. It is for this reason that small amounts of CNTs were incorporated into the polymer [3].

Since the first report in 1991 by Iijima, CNTs have been an area of intense research, hence their many applications. In this study the use of nitrogen doped CNTs (N-CNTs) as polymer stabilizers were exploited. The doping of CNTs with nitrogen leads to the following modifications on the surface: (i) high surface areas (ii) a high density of defects (iii) chemically active impurity sites (iv) unique inner closed shells in the CNT tube and (v) narrow tubes (the numbers of walls decrease with N inclusion) [16]. In addition to these mentioned modifications, nitrogen doping on the CNTs results to a change in chemical properties such as increase ability to functionalize their surface [16, 17] .

Dispersing Ag nanoparticles or metals on a solid support in general, has been based on conventional methods such as wet impregnation followed by chemical reduction, physisorption, radiolysis, physical evaporation, electroless deposition capillary action and solid-state reactions etc. [18]. These traditional methods have drawbacks such as lack of control on factors such as particle sizes and good dispersion [18, 19] .In addition, the multiple steps involved in these methods such as long ageing, drying and calcinations times make the process very slow and counter-productive. Thus, seeking alternative methods is crucial.

In this study, we report the synthesis, characterization and application of a two and a three component polymer nanocomposite materials namely N-CNTs/β-CD and Ag/N-CNTs/β-CD nanocomposites. These were synthesized by a microwave and a conventional *in-situ* polymerization method. The aim was to develop a green and more efficient procedure to synthesize these composites. To the best of our knowledge, the microwave-assisted method has not been used anywhere to prepare these polymers.

1.2 Justification

Waterborne diseases continue to be the leading cause of death worldwide. Diarrhoea alone for instance has been reported to kill millions of people every year, mostly children under age five [2]. Thus efforts to mitigate this problem cannot be overemphasised. The quality of our water is affected by both toxic and non-toxic species. Non-toxic pollutants alter the qualities of the water by introducing aesthetically undesirable problems such as colour, odour and bad taste [15]. Different treatment methods such as powdered activated carbon (PAC), ozonation, biological degradation and conventional methods such as flocculation, filtration, coagulation, sedimentation and disinfection have been used for taste and odour control but these methods fail to remove some of the organic pollutants from water at $ng \cdot L^{-1}$ levels [20]. The formation of disinfection by-product during water treatment by current disinfection methods is also the major limitation of their application. This calls for new methods that are effective in the treatment of water at the same time not compromising the health of individuals.

Polymer composites of cyclodextrin (i.e. N-CNTs/β-CD and Ag-N-CNTs/β-CD nanocomposites) have been reported to be effective in removing organic pollutants (at $ng \cdot L^{-1}$) and bacteria from water respectively. In addition, their advantage over conventional methods is that they do not produce any harmful disinfection by-products that are carcinogenic. Their structural integrity remains uncompromised even after a recycling for over 15 times, which means they can maintain their efficiency over a long period.

The synthesis of these polymer composites is still primarily based on conventional methods. This study reports on a greener and efficient way of synthesising these composites using microwave irradiation method. The method requires shorter synthesis times, produces high

yields, it is reproducible and no waste is generated thus making it environmentally friendly and viable.

1.3 Aim of the research study

The general aim of the research study was to synthesize novel CD polymers incorporating N-CNTs and Ag nanoparticles for water purification using a new method, **microwave irradiation.** The aim of the project was achieved through the following objectives:

- Synthesis of N-CNTs using a 10wt% Fe-Co/$CaCO_3$ catalyst in a CVD furnace.

- Functionalization and characterization of the N-CNTs.

- Synthesis of nanoporous polymer composites of β-CD incorporating N-CNTs and Ag nanoparticles (herein after referred to as N-CNTs/β-CD and Ag/N-CNTs/ β-CD) in a microwave.

- Characterization of the nanostructured materials using a range of techniques such as transmission electron microscopy (TEM), scanning electron microscopy (SEM), thermogravimetric analysis (TGA), Infrared (IR) spectroscopy, carbon-nitrogen (CN) analysis, X-ray photoelectron spectroscopy (XPS) and zeta potential measurements.

- Test of the nanotechnology-enabled porous nanocomposite systems for their capability to remove organic (*p*-nitrophenol, bisphenol A and trichloroethylene) biological contaminants from water.

1.4 Outline of dissertation

The succession and brief description of the chapters in the rest of the dissertation are given below:

Chapter 2 gives a detailed literature review of major aspects of the project such as priority organic contaminants, heavy metals and disinfection by-products. It also expounds on current and proposed water treatment methods etc.

Chapter 3 describes the experimental methods employed to achieve the objectives of the study.

Chapter 4 presents the results and discussion of the synthesized two component nanocomposites materials, N-CNTs/β-CD.

Chapter 5 presents the results and discussion of the synthesized three component nanocomposites materials, Ag/N-CNTs/β-CD.

Chapter 6 presents the conclusions drawn from the findings of this research. It also presents recommendation for future studies based on the conclusions that emanated from this study.

CHAPTER 2: LITERATURE REVIEW

2.1 Global water problems

Water continues to play a vital role in everyday living. It can be described as the very essence of life. Access to safe drinking water can therefore never be taken lightly. There are a number of factors that compromise the quality of drinking water. These include organics, inorganic and microbiological pollutants. The following section lists and explains some of the prominent pollutants, in particular the ones that are known to be priority pollutants in water.

2.1.1 Pollution by organic compounds

Organic pollution is a serious form of pollution. It poses serious health effects in humans. Over the years pollutants caused by organic pollutants have increased tremendously and this is due to the of use diverse chemicals in industry for the advancements of technology. Organic pollutants, whether harmless or toxic pose a negative effect on potable drinking water. Even when less toxic, some of these organic compounds carry with them undesirable properties such as odour, colour and bad taste [15]. Classes of organic pollutants include, natural organic matter (NOM) (e.g humic acid), phenols (e.g bisphenol A), dis-infection by products (DBP) (e.g. trichloroethylene), polychlorinated biphenyls (PCB) (e.g. naphthalene) etc. [12, 21, 22]. Many of the organic compounds are carcinogens and endocrine disruptors and their removal from water is crucial.

2.1.1.1 Natural organic matter (NOM)

NOM is a derivative of the degradation of naturally occurring material in water. It can be found in all surface, ground and soil waters. NOM covers a wide range of compounds from highly coloured, to aliphatic as well as charged and uncharged compounds with different chemical composition and sizes [21]. NOM is made up of hydrophobic and hydrophilic components with hydrophobic being the major fraction, making 50% of total organic carbon

(TOC). These include humic substances such as fulvic acid, humic acid and humin [21]. The hydrophobic substances are characterised by high aromatic carbon, phenolic structures and conjugated double bonds [23]. On the other hand the hydrophilic substances contain more aliphatic carbon and nitrogenous compounds such as sugars and carbohydrates etc. [21, 24]. Fig.1 shows structures of some the NOM found in water systems.

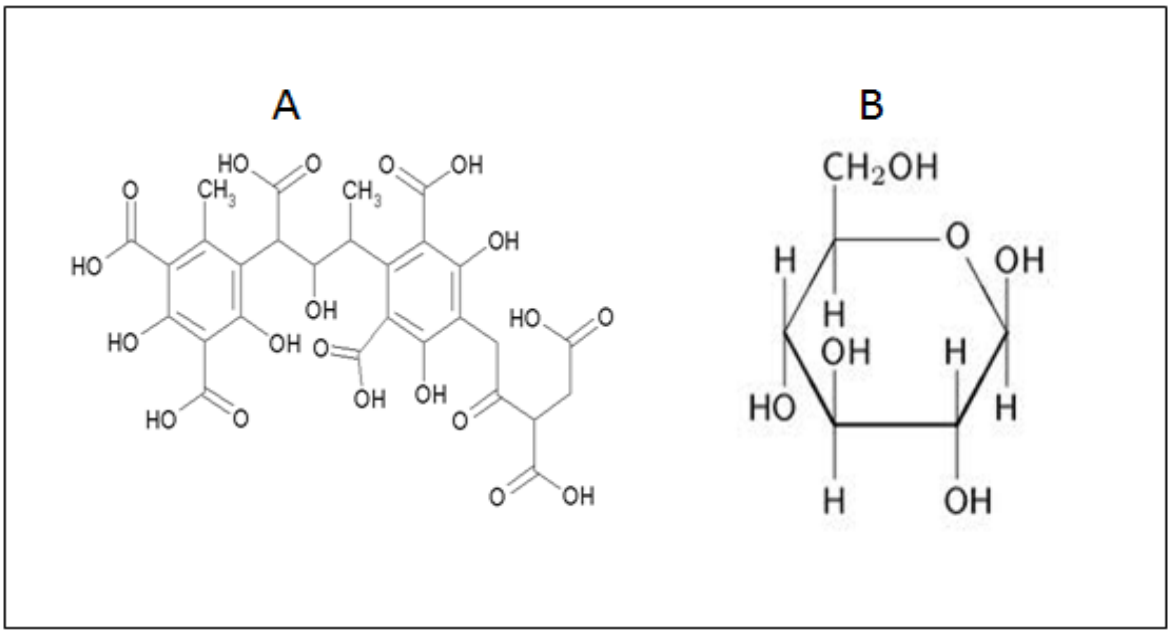

Fig. 1: Examples of NOM found in water: a) humic acid and b) glucose.

The pollution of water by NOM has increased significantly over the past 20 years. This is caused by the rise in air and surface water temperatures, an increase in rainfall intensity and decline in acid deposition etc. [21]. NOM itself is non-toxic, but its presence in water during water treatment especially when chlorine is present pose a serious problem due to the formation of BPs [15, 21, 25]. Non-toxic NOM also compromise the quality of drinking water by introducing colour, taste and bad smells [15, 21]. The removal of these materials in water is the crucial in order to eliminate secondary pollution.

2.1.1.2 Phenols

Phenols are aromatic compounds. They are widespread in aquatic systems due to their many commercial applications which dispose them as waste [26]. They are often produced as waste in pesticide manufacturing, coal power plants, petroleum industry, pulp, paper industry as well as plastic and pharmaceutical industries [22, 26, 27]. Phenols are known to be toxic

even at concentration levels as low as ngL^{-1} [26]. Also, small amounts of phenols that are present in water change the quality of water by introducing taste and odour. Two common examples of phenols present in water systems are described below:

a) P-nitrophenol

Paranitrophenol contains a hydroxyl and a nitro group in the 1, 4 positions of an aromatic ring respectively. They are widely distributed in the environment and they do not occur naturally in the environment but as waste products in the manufacturing of chemicals [28]. Their presence is solely a result of human activity [29]. Fig. 2 below shows a structure of *p*-nitrophenol.

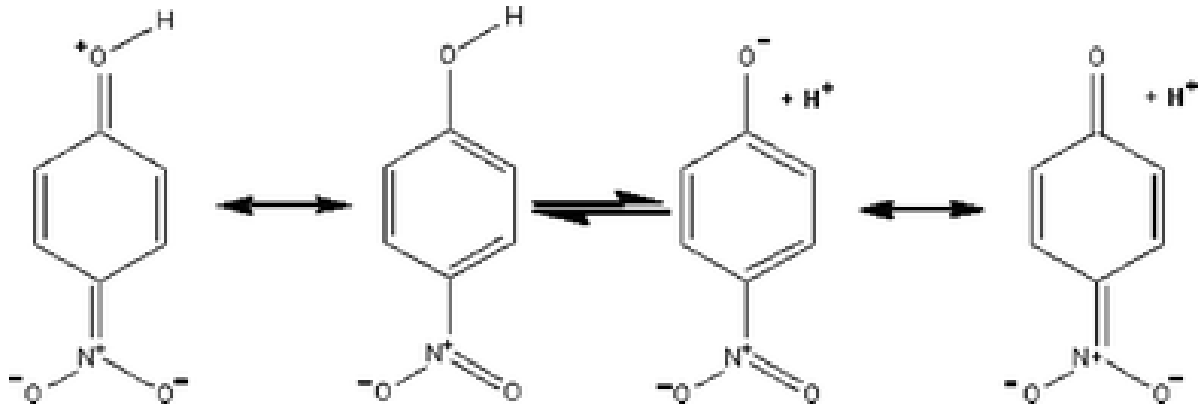

Fig. 2: The resonance structures of *p*-nitrophenol.

The wide distribution of *p*-nitrophenol stems from its many applications in agriculture, dyes, engineering polymers, and fungicidal applications for leather etc. [28, 29]. Exposure to *p*-nitrophenol results in a number of adverse effects on humans (e.g. anaemia, liver and kidney damage, skin and eye irritation etc.) [28]. High exposure to *p*-nitrophenol can cause blood disorder in which the blood losses its ability to transport oxygen to other tissues as shown by studies on animals [29]. This effect has not been reported for humans as yet but it is likely that exposure could cause similar effects.

b) Bisphenol A

Bisphenol A (BPA) is another high priority pollutant found in water systems. It is a reported endocrine disruptor that finds its way in the water systems as a manufacturing intermediate in polycarbonate, epoxy, polysulfone and other polymer resins [30-32]. Landfill leachates and wastewater treatment plants have been found as the principal route by which BPA enters the aquatic environment [32]. Bisphenol A has been shown to have oestrogenic activity which makes it a critical health threat [31]. It is for this reason that a number of treatment methods, chemical, physical and biological have been explored for the removal of BPA. The structure of bisphenol A is shown in Fig. 3.

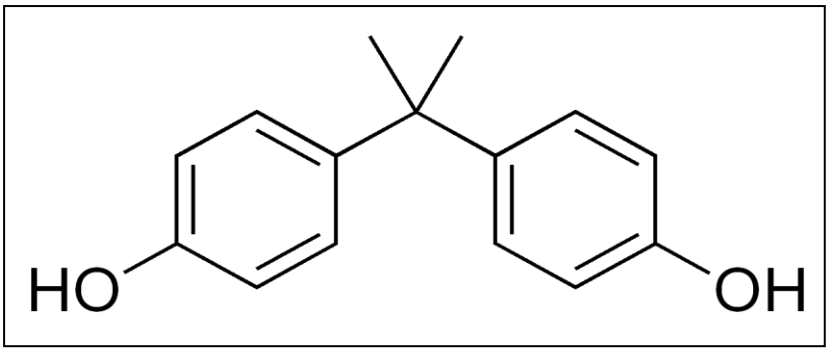

Fig. 3: Structure of bisphenol A.

c) Trichloroethylene

Trichloroethylene (TCE) is a volatile halogenated hydrocarbon compound. It is a common and persistent contaminant produced as an intermediate in production of polyvinyl chloride and fluorochemicals [33]. The applications of TCE involve its use as a metal greasing agent, historically as an anaesthetic and an antiseptic as well as a solvent for dry cleaning and coffee decaffeination [33, 34]. The presence of this compound in water systems has raised a lot of concerns regarding its health implications. Studies conducted have linked TCE to conditions such as cancer, congenital heart defects and spontaneous abortion etc. [33, 35]. The structure of TCE is shown in Fig.4.

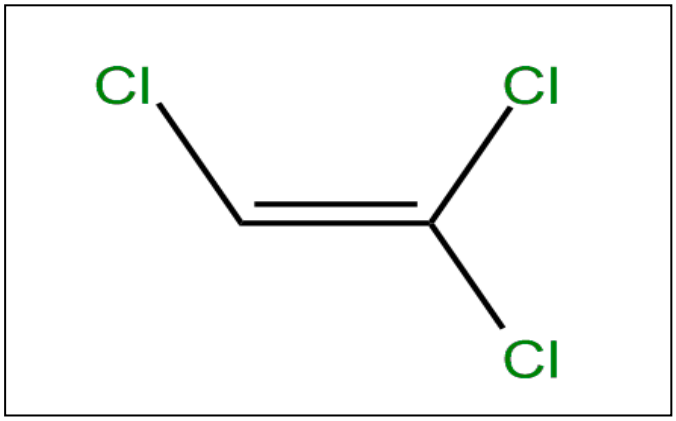

Fig. 4: The structure of trichloroethylene.

2.1.1.3 Water disinfection by-products

Current disinfection methods rely on chemical oxidants such chlorine, chloramines and ozone, etc. for water disinfection. As indicated in many publications, albeit being active in bacteria destruction, the secondary pollutants they produced by these methods are carcinogenic, mutagenic and endocrine disruptive [5, 36]. The by-products include compounds such as THMs, PCBs and haloacetic acids (HAA) that are formed when chlorine reacts with NOM (Fig. 5). Amongst these compounds, THMs and HAAs have been the area of focus because of their high abundance in chlorinated waters and because of their carcinogenic effects [36]. The regulation of these compounds in water is based on controlling the concentrations of dissolved organic matter (DOMs) in water before chlorination [37].

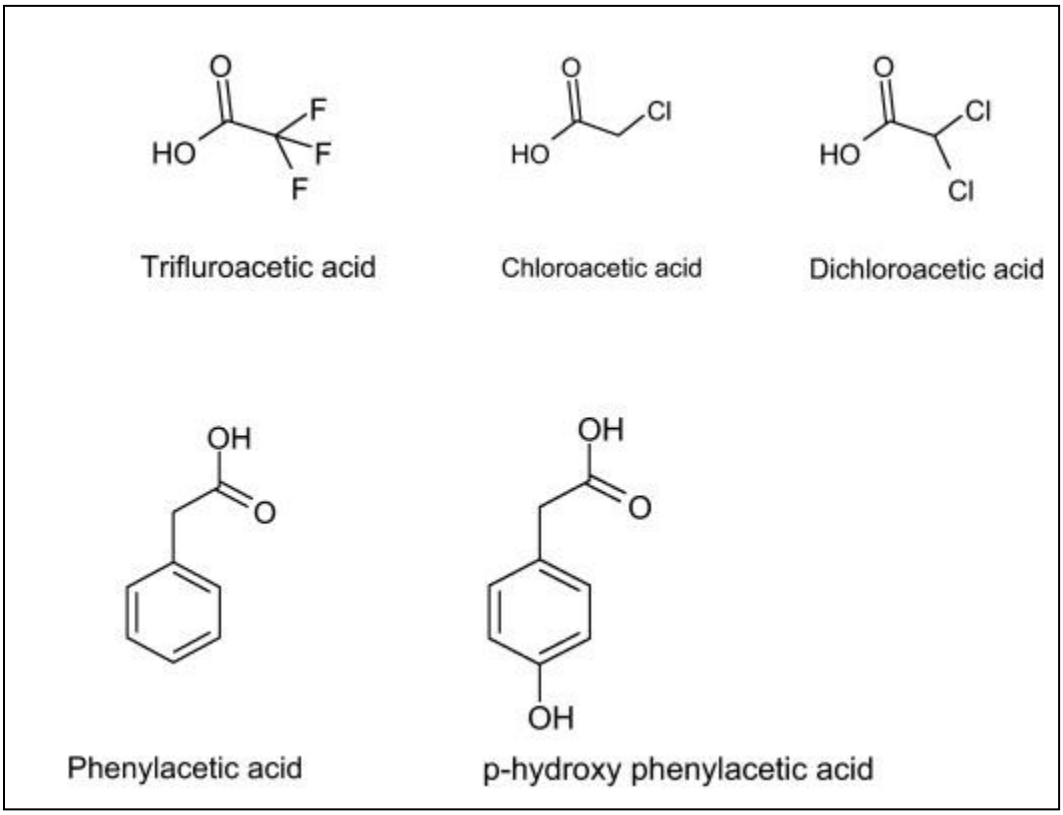

Fig. 5: The structures of different haloacetic acids found in water.

2.1.2 Pollution by inorganic compounds

In addition to organic pollutants, contamination of water by inorganic pollutants is a serious problem. Inorganic pollutants include heavy metals (e.g lead), metalloids (e.g arsenic), anionic pollutants (e.g perchlorates) and ammonia. These are found in water systems because they dissolve and get suspended in the water. The presence of these materials in water leads to adverse effects.

2.1.2.1 Heavy metals

The removal of heavy metals in water has been a serious problem for scientists for many years. Heavy metals have been considered as severe pollutants due to their high toxicity and their persistency [38]. Their presence in water systems occurs via a number of processes: through natural processes i.e. weathering and erosion of bed rocks and ore deposits etc.; and anthropogenically through mining, industries, agricultural activities and waste water irrigation [38-40]. Examples of toxic heavy metals in water systems include chromium (Cr) , zinc (Zn), lead (Pb), cadmium (Cd) and copper (Cu) [41]. Concentration levels of these

metal species have a direct effect on their toxicity. For instance, a specific level of Cr is needed for normal body functions; while its high concentration render this species toxic which can lead to liver and kidney problems [38]. Pb is also highly toxic and can cause severe health effects such as memory deterioration, and high exposure of it can further result in anaemia [38]. Zinc is also a species required by the body to maintain good function. The lack of it leads to poor wound healing, immune dysfunction etc. However, toxic Zn is detrimental as it cause sideroblastic anaemia [38]. These effects therefore place a huge emphasis on the concentration level control of these species in water systems.

2.1.2.2 Anions

Anions or oxyanions are another example of inorganic pollutants that are very toxic even at low dosages. Examples of these include arsenates ($H_2AsO_4^-$), perchlorate (ClO_4^-), chromates (CrO_4^{2-}) oxyanions etc., which make their way to water systems through anthropogenic activities such as mining, industry etc. [42]. Ferricyanide ($Fe(CN)_6^{3-}$), which is a source of cyanide is another example of oxyanions. It is very unstable and toxic. Its application includes their use as a cathode electrode [42-44]. The toxicity of these anions challenges the heath of all individuals utilising water systems infiltrated with this kind of contaminants.

2.1.3 Pollution by microorganisms

Another form of pollution that has raised a lot of health concerns is contamination by microorganisms. The WHO guidelines have stated microbial contamination to be the common and wide spread health risk associated with drinking water [45]. The presence of microbial agents in water has been associated with a number of waterborne diseases and these include outbreaks such as cholera, typhoid fever, bacillary dysentery, Cryptosporidiosis and Campylobacteriosis.

2.1.3.1 *Cryptosporidium parvum*

Cryptosporidium parvum is an intracellular protozoan parasite of the class Apicomplexa [46]. It is a coccidian parasite that reproduces both sexually and asexual, with the final stage of the life cycle occurring inside an individual host. Their primary source of transmission is

drinking water through oocsysts (thick-walled structure in which zygotes develop) they produce during reproduction, which are robust and can survive water treatment procedures [47]. They target primarily the epithelial cells of the gastrointestinal tracts in the host and results in profuse diarrhoea. Their infection can be very life threatening to immunocompromised individuals [47]. *Cryptosporidiosis* is the disease caused by *Cryptosporidium parvum* infection.

2.1.3.2 Escherichia coli

Escherichia coli (E. coli), a faecal coliform bacteria, is an anaerobic, gram negative bacilli found in intestinal tracts of humans and other warm-blooded animals [48]. It is used as a faecal indicator for the presence of pathogenic organisms and faecal materials of humans or other warm-blooded animals in water [48]. A number of factors are responsible for *E. coli* contamination and these include septic leachate, agricultural runoff and municipal waste water discharge [48]. The infectious dosage of *E. coli* for human is very low; a minimum of 10 cells is enough to cause illness. The outbreak of diseases such as haemorrhagic colitis and haemolytic uraemic syndrome have been attributed to the presence of *Escherichia coli* O157:H7 in the water [49].

2.1.3.3 Shigella spp

Shigella are gram-negative, rod-shaped, nonspore-forming and nonmotile bacteria belonging to the *Enterobacteriaceae* family [50]. The genus *Shigella* comprises of four species, *S. flexneri, S. sonnei, S. boydii, and S. dysenteriae*. *S. dysenteriae* is the one responsible for most reported epidemics because of their ability to produce toxins. Shigella is endemic worldwide with most cases of shigella infections reported in the developing countries [50]. A primary source of shigella is human faeces, hence their association with faecal contamination. It is mainly transmitted via water contamination. Shigella is responsible for the human condition *bacilliary dysentery*, an inflammatory disorder characterised by fever, intestinal cramps and blood stools [50].

2.2 Water treatment technologies

2.2.1 Conventional technologies

The contamination of drinking water by any of the pollutants already mentioned has critical impact on the health of any individual exposed to such kind of water. There is therefore a need for effective and efficient water treatment methods that will purify water. The importance of water treatment cannot be overemphasised considering that waterborne diseases continue to be the leading cause of death in developing countries [5]. The current water treatment methods employed are either through physical separation or chemical treatment. It is important to appreciate the importance of current technologies many of which have been used since ancient times. While they have been used for so long they have drawbacks that cannot stand the test of time.

2.2.1.1 Chlorination

Chlorination is a widely used disinfection method in developing countries [51]. It relies on the use of chlorine as a chemical oxidant for the destruction of pathogen and some organic and inorganic species in water. For instance nitrite reported to affect the oxygen absorption ability of the blood by combining with haemoglobin [52] can be oxidized to nitrates using chlorine. Chlorine has been found effective in the elimination of molds, algae and slime bacteria found occupying the walls of storage tanks and reservoirs [53]. The primary advantage of chlorine disinfection is that it leaves residual amounts that continue to help during distribution and storage. Chlorine is also a low-cost and versatile disinfectant [53]. However the use of chlorine also raises other health concerns; it is known to form disinfection by-products that are a serious health threats. Some of these problems (cancer causing) have already been explained in section 2.1.1.3 above.

2.2.1.2 Ozonation

Ozone is a powerful chemical oxidant used in the treatment of water. Although it is not as common as chlorine, the use of ozone as a disinfectant is increasing in the United States [54]. Ozone has a number of applications; amongst these is its use in the removal of DOM in

conjunction with biological treatment where ozone is used to transform DOM to biodegradable DOM [37]. Ozone's greater oxidation potential and the rapid decomposition of residual ozone in water has given it advantage over the other disinfection oxidants [54]. As with chlorine, the application of ozonation is limited due to the production of DBPs. For example, the presence of bromine ions in water result in their conversion to bromates which are known to be endocrine disruptive and carcinogenic [5, 55, 56].

2.2.1.3 Ultraviolet radiation

Ultraviolet light processes use UV radiation released from sources such as mercury and light emitting diode (LEDs) etc. for disinfection [57]. UV radiation is reported to be effective against micro-organisms by causing damage to their DNA, thus preventing replication of the microorganism. UV radiation also induces production of reactive species (hydroxyl radicals) from the water and organic matter present in it [58]. This in-turn oxidizes the membrane and proteins of the microorganisms. Wavelength normally used in UV process is 254 nm which is the DNA maximum absorption wavelength [57]. UV radiation has an advantage over the use of the other chemical oxidants in that it is cost-effective and does not produce secondary contaminants such as halogenated carbons and bromates which are reported endocrine disruptors and carcinogens [58, 59]. To enhance its efficiency, UV irradiation is normally coupled to with other disinfection methods such as chlorine and ozone etc. A drawback for using UV radiation is the lack of residual activity during treatments and the reported possible repair of UV-damaged organisms [60].

2.2.1.4 Granular activated carbon

Granular activated carbon (GAC) is made from carbonaceous materials such as wood, nuts, bone and coal etc. It can either be in powder form or pellets. The carbon is activated to increase its surface area. The high surface area of GAC has made it one of the best adsorbents for removing various contaminants from water. GAC has been widely used in the removal of organic contaminants from wastewater and drinking water due to its strong affinity for organic compounds even at very low concentration levels [61].

Although GAC has high adsorption capacity, it can only maintain this for a short period after its active sites have been occupied with organic pollutants [61]. With treatment, the active sites for adsorbing the pollutant decreases. This raises a need to regenerate it. Reports have shown that the adsorption capacity of this material decrease with each regeneration cycle. This has made the process to require much capital investment and operating costs [62]

The advantages and disadvantages of the conventional technologies used in water treatment are summarised in table 1 below.

Table 1: Advantages and disadvantages of the various conventional technologies in water treatment:

Technology	Advantages	Disadvantages
Chlorination	- Eliminates molds, algae and lime bacteria - It leaves residual amounts that continue to help during distribution and storage - It is low cost	- It produces disinfection by-products that are carcinogenic
Ozonation	- Efficient in removal of Dissolved Organic matter (DOM) - Has greater oxidation potential than other disinfection oxidants	- Produce DBPs which are endocrine disruptive and carcinogenic.
Ultraviolet radiation	- Effective against micro-organisms - Cost-effective and does not produce secondary contaminants	- Lack of residual activity during treatments resulting in UV-damaged organisms repairing
Granular activated carbon	- High surface area provides efficient removal of various contaminants from water - Has strong affinity for organic compounds even at low concentrations	- Can only maintain its high adsorption capacity for a short time after active sites are occupied - Adsorption capacity of the material decreases with every regeneration cycle - high capital investments and operational costs

2.2.2 Technologies based on nanostructured materials

Due to increase in human population, a lot of pressure is exerted on water sources to meet water demands. Pollution of water sources has magnified the problem of clean and safe drinking water supply from current sources. The failures and the health implications of most of the current disinfection technologies have placed a need to re-evaluate current disinfection methods and to look into innovative approaches that not only effectively remove pollutants from water but also do not compromise the health of individuals. Nanotechnology based water treatment methods can make more efficient alternative disinfection techniques. They can be used solely or be used in conjunction with some of the current disinfection technique such as UV disinfection [5]. The application of nanotechnology based water treatment methods can also revolutionarize water disinfection as we know it, by providing an opportunity to switch from centralised to decentralised or point-of-use water treatment systems [5]. A brief discussion of current and emerging nanomaterials based technologies for water treatment are discussed. Emphasis is placed on polymer nanocomposites for water purification.

2.2.2.1 Membrane technologies

Membrane based technologies for drinking water and waste water treatment, as well as sear water desalination are considered very important components of modern day water treatment [63]. The main advantages of membrane processes are their production of clean water in just one purification step and their upscalability. Membranes can be applied at any stage of emergency and at any intervention level [64].

There are a number of driving forces in membrane-based separation technique such osmotic differences, pressure and temperature. These are used to classify the type of membrane separation [64, 65]. The pressure-driven membrane processes are classified into microfiltration, ultrafiltration, nanofiltration and reverse osmosis (RO) based on the membrane pores size [64, 65]. An example of microfiltration membrane filters is ceramic filters which have been reported to have considerable removal of *E. coli* and other bacteria from water. However, their low throughput of water limits their application. Ultrafiltration, commonly used in disaster relief, displayed excellent rejections against bacteria and viruses. For multivalent ion rejection and some organics, nanofiltration is employed. Their application

in water desalination is not solely but in conjunction with other processes. RO processes have high rejection for a number of contaminants including radionuclides etc. [66]. Their application is limited by high energy consumptions [64].

For osmotically-driven processes, a forward osmosis (FO) process, which can achieve high rejection for a wide spectrum of contaminants similarly to RO but with no pressure is applied [67]. The application of FO might be limited due to the fact that it produce sweetened water and can be prone to bacterial re-growth.

Thermally-driven membrane processes include membrane distillation. This process is based on three steps: (i) evaporation of water on the feed side; (ii) migration of water vapour to the permeate side via membrane pores; and (iii) condensation of water vapour on the permeate side [68, 69]. This process is driven by vapour pressure differences as a result of temperature gradient between feed and permeates side [64, 68].

With all membrane based process, the major problem limiting their application is fouling by organics and biofoulants etc. There are now attempts to mitigate this problem of fouling and one of the ways is to integrate the membrane system with nanomaterials such as carbon nanotubes, nanoparticles (e.g. Ag), zeolites and dendrimers etc. These are reported to improve cost-effectiveness and the filtration process. The impregnation of photoactive nanomaterials renders the membrane reactive and not just be a physical barrier and achieving multiple treatment goals with minimisation of fouling [64].

2.2.2.2 Noble metal nanoparticles

The use of metal nanoparticles is one of the many other steps taken to switch the dependence of water treatment on conventional methods. The use of metals in disinfection is of ancient origin. Silver and gold have been used back in the day for preservation of perishables and disinfection of water [1]. The many applications of these metals and other transition metals such as copper and iron were based on their macroscopic structure. In terms of applications, nanosized form of these metals such as zero-valent iron nanoparticles (ZVI), Ag nanoparticles, gold nanoparticles and copper nanoparticles etc. have had advantages over their macroscopic counterparts due to their improved surface area and surface energy [70]. In our study Ag nanoparticles was chosen for the destruction of *E. coli.*

Ag is a transition metal whose application dates back in ancient times. Ag has been used domestically for lining of many utensils. A lot of vessels have also been made based on Ag for storage of wine and perishables. It was in the years 1869 and 1893 that pioneering work on antibacterial properties of Ag was done [1]. It was reported that Ag salts displayed antibacterial activity against *spirogyra* (1869) and *aspergillus* spores (1893) respectively [1]. The 20th century marked also the use of silver based water filters for action against bacteria [1].

Ag nanoparticles have also been reported to be effective biocides. There are a number of Ad nanoparticle based purification systems that have already been commercialised such as Aquapure®, Kinetico®, and QSI-Nano® [5]. These systems have displayed 99.99% removal of pathogenic bacteria, protozoa and viruses etc. [5]. However, to this date, their mechanism of toxicity is only partially understood. Ag ions are reported to interact with the thiol groups in proteins which result in inactivation of respiratory enzymes and leading to production or reactive oxygen species (ROS) which are detrimental to cell function [2]. Also, Ag^+ ions prevent DNA replication and destruct the cell membrane which results in loss of permeate selectivity [2].

The Ag nanoparticles have also displayed some antibacterial activity and their mechanisms of destruction are postulated as follows: (1) Ag nanoparticles adhere to the cell membrane surface and cause alterations by forming pits which then results in increase in membrane permeability, (2) Ag nanoparticles also penetrate the inside of the bacterial cell and cause DNA damage and (3) dissolution of Ag nanoparticles releases antimicrobial silver ions (Ag^+) [2]. Fig. 6 shows a summary of some of the mechanisms displayed by the nanoparticles in destructing bacteria.

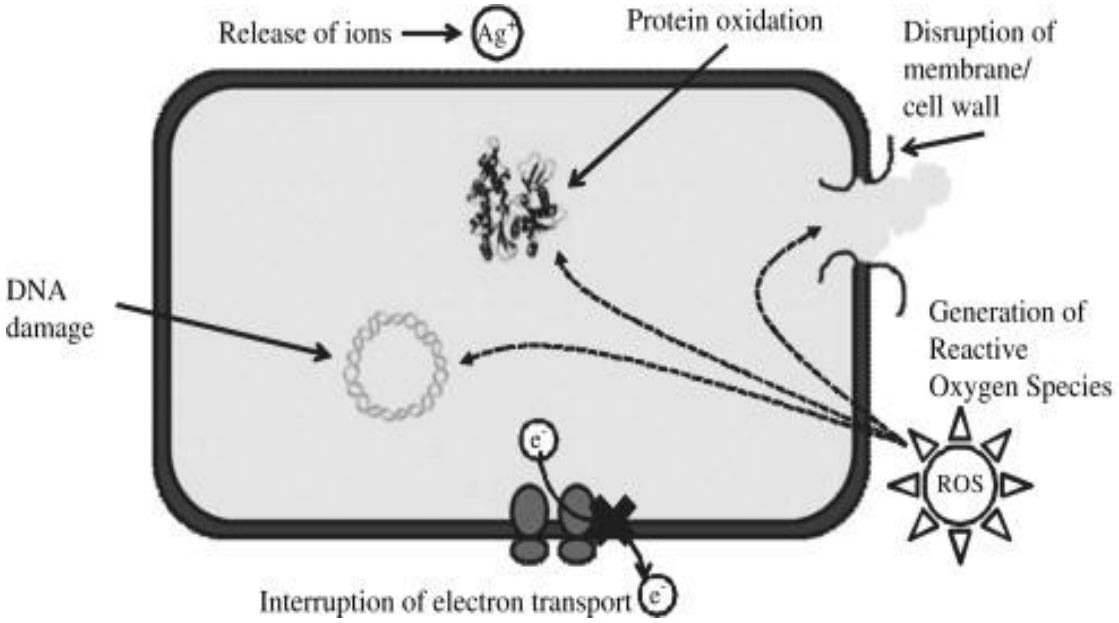

Fig. 6: Various mechanisms of antimicrobial activities exerted by nanomaterials [2].

The antibacterial activity of the Ag nanoparticles is based on the physicochemical properties such as size and shape. Ag nanoparticles of less than 10 nm display excellent toxicity against bacteria. The nanoplate forms of Ag nanoparticles also display more toxicity than nanorods or nanospheres etc.

2.2.2.3 Polymer nanocomposite materials

The application of polymers in stringent conditions is limited due to their compromised structural stability [71]. For this to be circumvented, various inorganic materials can be incorporated in the polymer matrix, and depending on the type inorganic material, the application of the nanocomposite will vary. Their nanoscaled dimensions provide the composite with special and unique properties which cannot be provided by their microscope counterparts such as stiffness and strength etc. [72].

(a) Polymer-clay hybrid nanocomposite

Clay nanolayers (layered silicates) make excellent inorganic reinforcements in many polymer matrix. There are three classes of polymer-clay composites namely conventional composites, intercalated nanocomposites and exfoliated nanocomposites and these vary based on position

and arrangement of the clay relative to the polymer [73]. For conventional composites, the polymer matrix is not intercalated into the clay as opposed to the intercalated nanocomposite where the polymer is inserted into the clay structure. For exfoliated nanocomposites, the clay layers are separated by a continuous polymer matrix that depends on loading [73]. The loading of clay in polymers produce a wide spectrum of nanocomposites with improved properties. Polysiloxane elastomers reinforced with nanosized silica particles showed improved thermal stability and reduced solvent uptake [74]. Also, the incorporation of clay nanolayers in elastomeric epoxy has been shown to improve drastically the toughness and tensile properties of these thermoset systems [73]. Many of these improved properties rely heavily on the dispersion of these reinforcers within the polymer matrix. Excellent dispersion of the silica layers is therefore required for efficient reinforcement of the nanocomposites [74].

(b) Chitosan

Chitosan is derived from natural sources such as crustaceans, fungi and exoskeleton insects. It is an artificial variant of chitin. Their polymers are semi-synthetically derived amino polysaccharides that possess unique structures and many properties that give them vast applications in biomedical and other areas of industry [75]. Chitosan's biocompatibility and excellent biodegradability renders them non-toxic and very safe for their application [76]. They have useful activities that are antifugal, antibacterial and antitumor [75].

(c) Cyclodextrin polymers

Cyclodextrins (CDs) are cyclic oligomers formed from the 1, 4 linkages of glucose units. Their synthesis is based on enzymatic degradation of starch by a CTG-ase enzyme produced from a number of microorganisms such as *Bacillus macerans etc.* [77]. CDs are a class of three cyclic oligosaccharides which differ on their number of the glucopyranose units in the cyclic chain i.e. 6 glucopyranose units for α-CD, 7 glucopyranose units for β- CD, and 8 glucopyranose units for γ-CD [77] (Fig. 7).

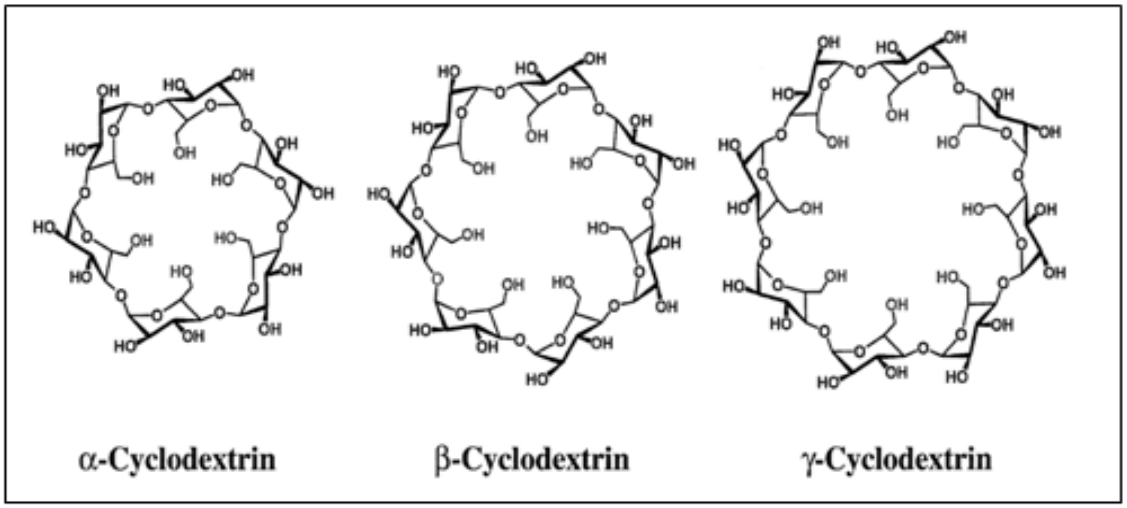

Fig. 7: Structures of the different CDs showing different numbers of glucopyranose units forming the cyclic oligomer.

In a 3-dimensional view the CDs have a circular, conical conformation with a height of 8 Å and inner diameter of the cavity ranging between 5- 8 Å [78]. The diameter is dependent on the number of glucopyranose units in that particular cyclodextrin, with larger diameters possessed by CDs with more glucopyranose units. The three CD classes exhibit different physical properties and some of these are summarised in Table 2.

Table 2: Characteristics of α, β, γ cyclodextrin [77]

Property	α	β	γ
Number of glucose units	6	7	8
Molecular weight (g/mol)	972	1135	1297
Solubility in water, g/100 mL at room temp	14.5	1.85	23.2
Cavity diameter, Å	4.7-5.3	6.0-6.5	7.5-8.3
Height of torus, Å	7.9	7.9	7.9
Diameter of outer periphery, Å	14.6	15.4	17.5
Approximate volume of cavity, Å	174	262	427

The CD structure bears hydroxyl groups that influence the cone shape that it displays. The wider end of the CD bears secondary hydroxyl while the narrow end bears primary hydroxyl.

It is the free rotation of the latter that reduces the diameter of the cavity [77]. A schematic representation of CD showing the primary and secondary hydroxyl groups is shown in Fig. 8.

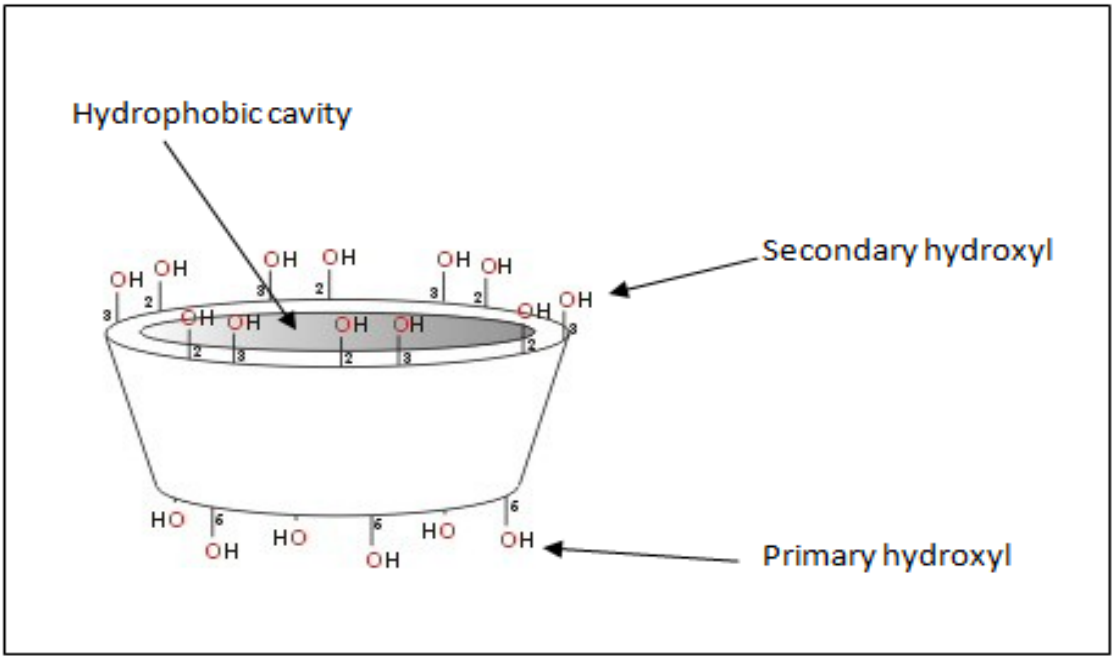

Fig. 8: Schematic representation of β-CD indicating the different hydroxyl group in the structure.

The structure of CDs makes itself ideal for their interaction with organic molecules. The presence of hydrogen and carbon in the interior creates a hydrophobic environment whilst the oxygen of hydroxyl groups in the exterior creates a hydrophilic environment. Although this structure is ideal for interactions with organics, their hydrophilicity renders them soluble in water thus not making them suitable for water treatment without modification or polymerizing them.

(c) Cyclodextrin inclusion complexes

The various applications of CDs in water treatment and in drug delivery are based on their ability to form guest-host complexes. The driving force for such complex formation is the substitution of high enthalpy water molecules in the interior of the CD cavity (apolar) by an appropriate guest molecule [77]. In an aqueous medium, the interior of the CD is unfavourably occupied by water molecules (polar). This creates unfavoured interactions, polar-apolar interactions. Since this type of interaction is not favoured, the water molecules

can be readily substituted by an appropriate guest molecule [77]. CDs can encapsulate various small organic compounds with suitable geometries into their cavity [79]. The principal factors that are responsible for binding between the host and guest are primarily van der waals and hydrophobic interactions [80]. The simplest host: guest ratio that exists during complexation is 1:1. However other complex ratios have been reported such as 2:2, 1:2, 2:2 etc. Fig. 9 is a schematic showing inclusion complex formation in aqueous region.

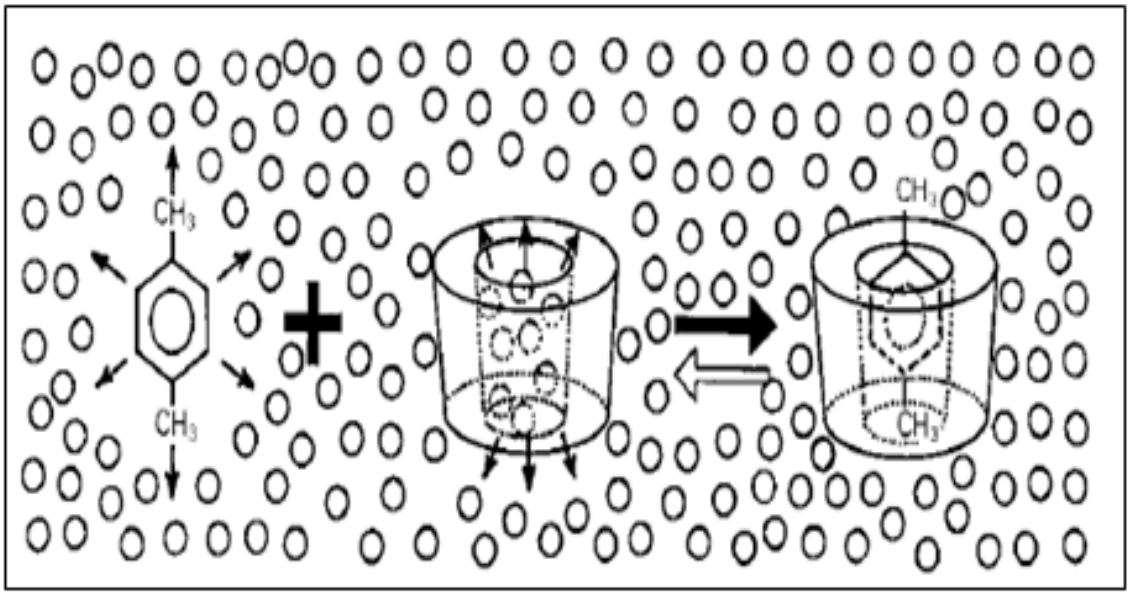

Fig. 9: Schematic representation of CD-guest complex formation in water.

(d) Cyclodextrin polyurethanes

The application of CDs in water treatment is achieved by making the CDs insoluble by forming polymers [79]. The polymerisation of CDs takes advantage of the reactivity of the exterior hydroxyl groups of the cyclodextrin. Polymers of CDs can be formed by polymerisation of CDs with a number of linkers such as hexamethylene diisocynate (HMDI) and toluene 2,4 diisocyanate (TDI) (Fig. 10). This polymerisation process renders these polymers insoluble in water. Tested polymers of this material have been reported to be effective in removal of organic pollutants from water [81]. Below is a reaction scheme for the polymerisation of CD with diisocynate linker.

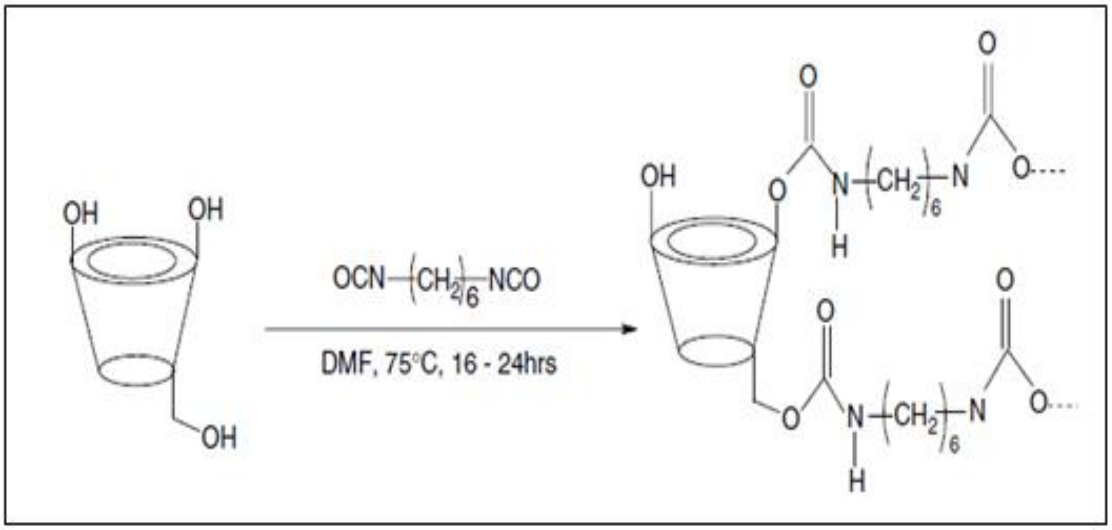

Fig. 10: Synthetic pathway for cyclodextrin polyurethanes [15].

2.3 Adsorption capacities of various media for removal of phenolics

Previous sections have demonstrated the negative impact that organic pollutants, particularly phenolics have on human health. Phenolics which make their way to water streams through production activities i.e slimicide production, disinfectant, and antiseptic production etc. pose a serious health threat and their presence in water is crowned an important environmental issue [22, 26, 27]. There are a number of techniques that are employed for the removal of phenols in water. Table 3 highlights some of the commonly used adsorption techniques and their corresponding adsorption capacities for para-nitrophenol removal. It must be kept in mind that adsorption capacities will vary with varying experimental conditions.

Table 3: Adsorption capacities of various adsorption media for removal of *p*-nitrophenol in water [27].

Adsorbent	Adsorption capacity (mg/g)
Bagasse fly Ash	8.3
Residual samla coal	86.9
Commercial activated carbon	526.3
Silica beads	116.1
Charred sawdust	147.0

Cyclodextrin-based polymers as opposed to adsorbents absorb organics into their cavity thus forming a host: guest complex [79]. This allows the organics to be transported within the bulk of the nanoporous polymers thus making the polymers to have a loading capacity comparable to activated carbon even though they have drastically different surface areas, 1- 2 m^2/g for cyclodextrin and 600 m^2/g for activated carbon [79]. The cyclodextrin-based treatment system is a viable choice over the other techniques in that it allows for removal of organics even at lower concentration level, ng/L, were the other techniques fail to do [15, 79].The incorporation of Ag nanoparticles in the CD polymers system provides the system with antibacterial activity. This gives the cyclodextrin-based system a multi-treatment ability in that it is able to remove organic pollutants and at the same time destroy microorganisms.

2.4 Carbon nanotubes and doped carbon nanotubes

Since their discovery by Iijima in 1991, carbon nanotubes (CNTs) have been an area of intense research, hence their many applications today. CNTs are allotropes of carbon in the sp^2 hybridisation state with cylindrical shape [82]. There are two main types of CNTs and these are distinguished from each other by the number of graphitic sheets they contain. Single-walled carbon nanotubes (SWNTs) are the simplest of the two carbon structures with only one graphitic sheet folded to give a cylindrical shape. Multiwalled CNTs (MWCNTs) contain an array of these graphitic sheets folded to give the same cylindrical shape [83]. Different physical characteristics of CNTs such as diameter and length of tubes have been reported and these were fundamentally related to the experimental condition of synthesis such as catalytic cracking of the hydrocarbon gases [84]. The diameter of MWNTs ranges from ~ 4 to 100 nm and that of SWNTs from ~ 0.4 to > 3 nm. The properties of the carbon nanotubes can be changed by tuning their diameters [85]. Fig. 11 shows the structure SWNTs and MWNTs.

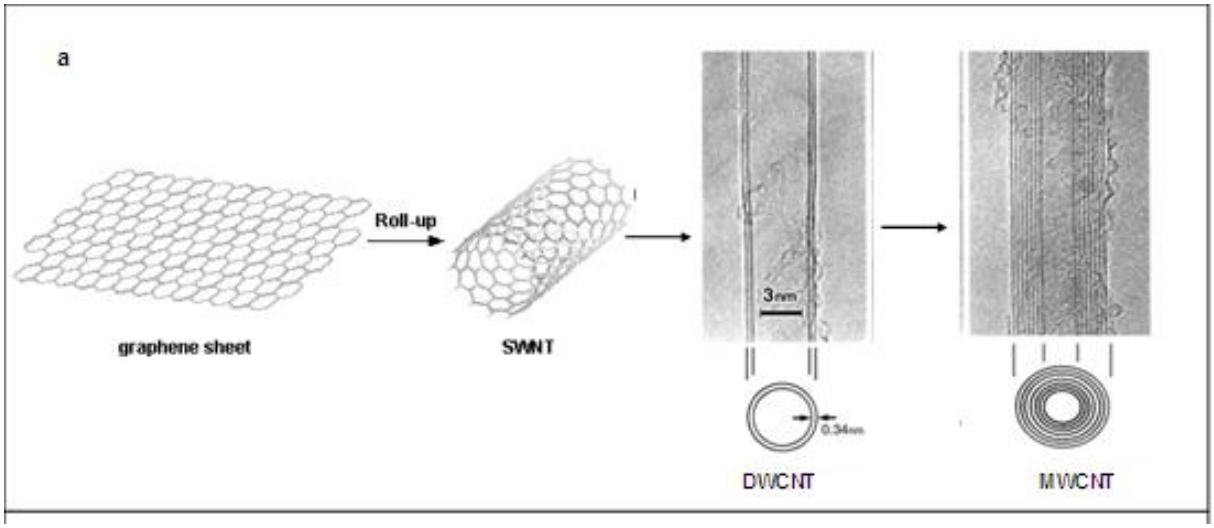

Fig. 11: Structures of a graphene sheet, single-, double-, and multi-walled CNTs.

CNTs possess unique structural, physical and electronic properties. Pristine CNTs have been reported to be very conductive. Because of their one-dimensional nature, charge carrier travel in the tubes without experiencing any scattering which means Joules heating is minimized thus increasing the amount of current density the tubes can carry [83]. The exploitation of the CNTs' properties has also resulted in many applications of these materials in industry such as conductive and high-strength composites, hydrogen storage and energy conversion devices [85]. Their improved surface area has made them good adsorbents for toxic metals and organics in water. They are also used as substrates for metal dispersion for applications in catalysis and water treatment etc.

The morphology as well as the physical properties of the CNTs are dependent on the synthesis technique [84]. A number of techniques are used for the production of CNTs such as carbon-arc discharge, laser ablation and chemical vapour deposition (CVD) etc. [85]. CVD is the most common and widely used synthesis method due to its ability to produce large quantities of tubes at a relatively low cost [83]. The technique relies on the use of transition metals such as Fe, Co, Ni etc. as catalyst for the CNT synthesis. After synthesis, the product is usually acid treated to remove impurities and the catalyst remaining after production. The inability to remove completely the catalyst residues is a major drawback for the CVD [83].

CNTs are generally inert and insoluble in aqueous and most organic solvents. Introduction of acid functional groups and other heteroatoms in their structure renders them reactive [86]. The introduction of these groups can be covalent, non-covalent or by the filling of their

cavity. Functionalization of CNTs opens a new area of nanotubes/polymer composite. The insolubility and lack of compatibility of unfunctionalized (pristine) CNTs with the polymer renders them difficult to use in polymer nanocomposites since they lack good dispersion and homogeneity. However after modifying the surface, improved dispersion can be achieved [86]. Functionalization of the CNTs also improves the dispersion of metal nanoparticles on their surface.

The insertion of heteroatoms like nitrogen (N) into the CNTs lattice has been shown to alter the overall structure of the CNT which results in different physical and chemical properties [16]. The introduction of a heteroatom into the CNTs can be done in a number of ways such as during gas phase reactions using ammonia, or by adding nitrogen to the carbon source or to the catalyst ligands when using a gas phase/floating catalyst [87]. The insertion of N atom into the CNTs' lattice changes the symmetry and hence the structure of the CNTs. The mechanical strength and electrical properties of the CNTs were also reported to be affected by doping. With the incorporation of just small amounts of N into the CNTs, the electronic properties can be significantly altered. This is because N has one extra electron than C, so its substitution for carbon would result in novel electronic properties [17]. This is one of the ways considered for fine-tuning electronic properties of CNTs [16].

The substitution of C in the graphitic lattice is not the only way to incorporate N in the CNT assembly. Other ways include incorporation on the walls of the tubes. Due to its size, the N can generate a defect in the tube structure keeping the N atoms on the walls with the rearrangement of the neighbouring carbon atoms [16, 17]. Besides the two on-wall-dopants, some of the atoms can also be encapsulated in the hollow core of the tubes (endohedral doping) or trapped within bundles intercalated between the outer shells of the tubes (exohedral doping) as shown in the Fig. 12.

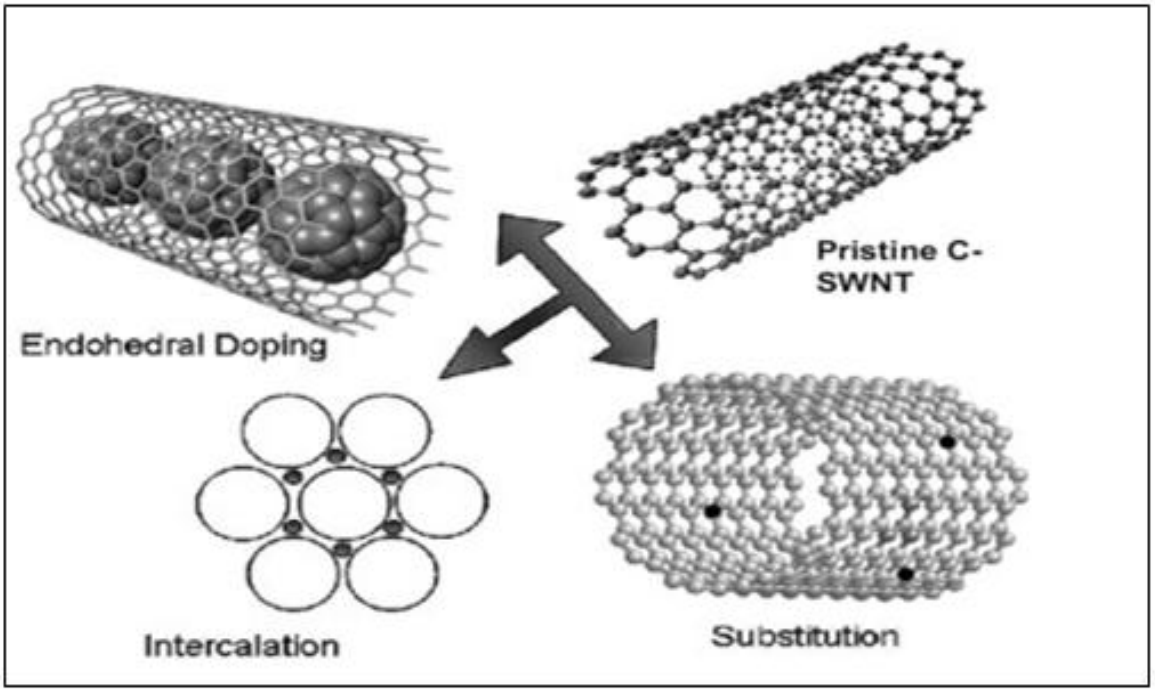

Fig. 12: Different ways to modify nanotube electronic properties [16].

Doping with N also improves on the surface reactivity of the CNTs. The N sites of the CNTs have been shown to anchor the metal on CNTs leading to excellent dispersion in the metal/CNTs hybrid material [16]. Excellent metal dispersion and narrow particles size distribution of metal nanoparticles in the metal/N-CNTs is good for enhanced antibacterial activity by these hybrid material in the polymer composite reported in this study.

2.5 Green chemistry

With the advancement of technology, ways to synthesize various materials have improved signicantly. The chemical industry has played a very pivotal role in improving the quality of life in both developed and developing countries. The innovation technologies that led to life-saving medicines, and fertilizers used in the alleviation of hunger etc. have greatly impacted our lives [88]. These chemical and many other essential products continue to be produced as man-kind continue to exist. The production of these products for development and improvement of life have resulted in environmental and local populations being affected.

With the need to improve the quality of life while not compromising the health of human and the environment, green chemistry and engineering arise as a bridge to reconcile the

production of the essential products while reducing the production of waste [88]. Green chemistry is defined as the design of products and processes that eliminate the use and generation of hazardous substances [88, 89]. The need for greener technologies cannot be overemphasized. These will be important alternatives for development with the potential to be sustainable since they will not compromise the heath of both humans and the environment. The idea was to apply some of the twelve principles of green chemistry in synthesizing some of our nanocomposites materials.

2.6 Microwave synthesis

In synthetic chemistry, time is valuable because of a lot of time is spent on trial and error experiments to develop new synthetic routes or to optimise already existing protocols with respect to product quality and yields etc. With the newly emerging and developing field of nanotechnology, a lot of time is spent on developing robust synthetic routes for many of the nanomaterials. Reproducibility tests then become a critical part of the development and increased expansion of such a technology. The development of synthetic techniques that will be environmentally friendly, time efficient and ones that will improve on the quality of results is inevitable.

Microwave irradiation as a fast synthesis technique that has become an indispensable tool in modern organic chemistry since the first report of its use in 1986 [90]. Pioneering work in the field of microwave synthesis was done on a domestic microwave oven. This raised a serious issue of safety since there were no sensors for pressure and temperature monitoring. Nowadays industrial microwaves are utilised. These have a built-in magnetic stirrer, different probes for pressure and temperature monitoring [90, 91]. The microwave reactors are in contact with sensors that are able to regulate the pressure and temperature by adjusting the power output [90, 91].

Microwave radiation is an electromagnetic radiation in the frequency range 0.3- 300 GHz corresponding to 1mm to 1m wavelengths [91]. Kitchen microwaves and commercial microwave reactors use frequencies of 2.5 GHz. The rest of the microwave radiation spectrum is ascribed to telecommunication and radar technology [90, 92]. Microwave chemistry is based on the ability of a material to convert microwave energy to heat

(dielectric heating) [93]. As opposed to processes such as photochemistry, microwave irradiation does not induce chemical reactions but rather efficient heating of a material. The energy of a microwave photon at 2.45GHz is about 1 J mol^{-1} which is much too low to cleave chemical bonds, a requirement for chemical reaction [90] . Microwave heating is reported to occur in two mechanisms i.e dipolar polarisation and ion conduction. The polarisation mechanism occurs only when the irradiated material has a dipole moment. Due to its sensitivity to the electric field, the dipole will try and align itself with the field by rotation [18] . Collisions of the molecules occurs as the molecules try and follow the field resulting in heating being observed due to friction [90, 94]. The other mechanism, conduction, is a much stronger interaction compared to dipole polarisation in terms of their heat-generating capabilities [18]. It is based on the charged materials in the heated material. Mobile charge carriers (electrons, ions, etc.) move relatively easily through the material under the influence of the microwave's electric field. These induced currents will cause heating in the sample due to any electrical resistance [18, 94].

Two factors are used to define the dielectric properties of a material: (1) dielectric constant ε′, describing the ability of the material to be polarised by the electric field and (2) dielectric loss ε″, which indicates the efficiency at which the material converts microwave energy to heat [90, 94]. The ratio of the two gives rise to the loss factors $\tan \delta = \varepsilon''/\varepsilon'$ which describes the ability of the material to convert electromagnetic radiation to heat [93]. Materials like organic solvents (e.g ethylene glycol) which are high microwave absorbing solvents have a loss factor greater than 0.5 ($\tan \delta > 0.5$) whereas medium and low absorbing solvents (e.g acetonitrile) have values of 0.1– 0.5 and < 0.1, respectively [90].

Microwave irradiation provides a number of advantages compared to the conventional method. It is known to be energy effective since it directly heats the mixture as opposed to the conventional were the vessel is heated first then the heat is transferred to the bulk via convection [95, 96]. Microwave irradiation provides rapid heating rates and temperature homogeneity while the conventional methods are characterized by slow heating rates and increased thermal gradients [96-98]. Microwave irradiation can also achieve volumetric heating throughout the volume of the material since it can penetrate the core of the bulk solvent and supply energy [94]. Microwave irradiation also leads to high product yield due to the elimination of secondary reactions because of the selective heating provided by the microwaves [98]. The synthesis of nanoparticles whose growth is highly sensitive to reaction

conditions will benefit from the homogenous and efficient heating provided by microwave irradiation [90].

CHAPTER 3: EXPERIMENTAL

3.1 Synthesis of catalysts

A method by Mhlanga and co-workers was adopted for the synthesis of the 10 wt.% Fe-Co/$CaCO_3$ catalyst [99]. Calculated amounts of Fe and Co sources, $Fe(NO_3)_3{\cdot}9H_2O$ (7.24 g) and $Co(NO_3)_3{\cdot}6H_2O$ (4.94 g) were first dissolved in 100 ml of distilled to make the solution as dilute as possible to produce very small particle sizes of the catalyst. The solution was then added slowly while stirring into a beaker containing 20g of calcium carbonate ($CaCO_3$), a solid support which aids in the dispersion of the metal particles. The solution was allowed to stir for several minutes after which the contents were filtered and allowed to stay overnight in a ventilated fume hood. The catalyst was then ground to fine powder and screened using a 150 μm sieve. The powdered catalyst was then calcined in a furnace at 400 °C for 12 h to remove the nitrates.

3.2 Synthesis of N-CNTs

The synthesis of the N-CNTs was achieved via a modified chemical vapour deposition (CVD) method (Fig. 13), using the 10 wt.% Fe-Co/$CaCO_3$ catalyst [99, 100]. 0.3 g of the 10 wt.% Fe-Co/$CaCO_3$ catalyst suspended in a boat was placed inside a furnace heated at 700 °C. Flow rates of the carrier gas (nitrogen) and the carbon source (acetylene) were adjusted to 240 ml/min and 90 ml/min respectively. This mixture was then bubbled through acetonitrile (nitrogen source) into a quartz tube containing the catalyst. The gases were allowed to run for 1 h and the synthesized carbon material was collected in the boat. After the run acetylene was switched off and the nitrogen gas was allowed to run while the system cooled. The Fe-Co/$CaCO_3$ catalyst has been reported to give high yields of N-CNTs and it is relatively easy to remove it using mild acids and thereby attain high purity N-CNTs [99, 101-103].

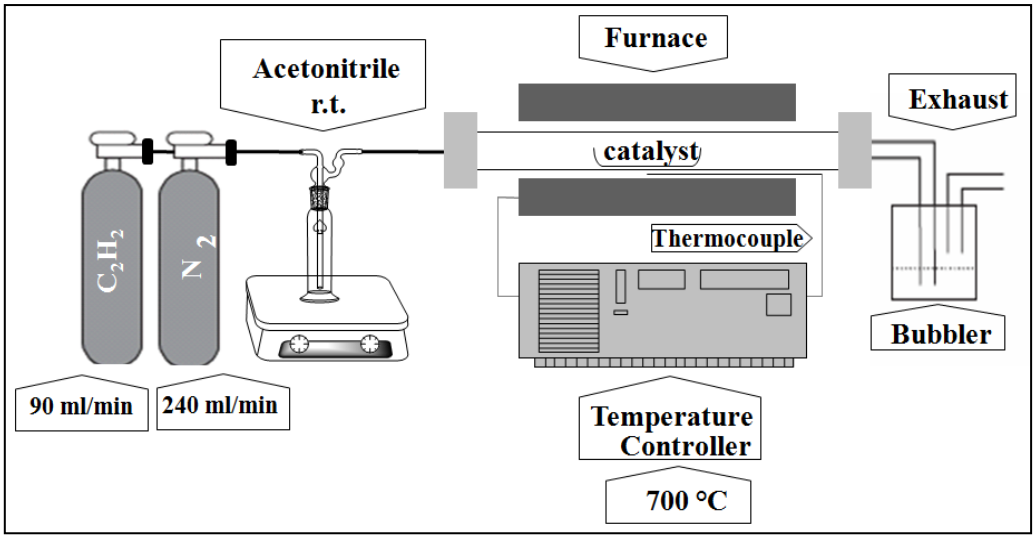

Fig. 13: Chemical vapour deposition set-up for the synthesis of N-CNTs

3.3 Conventional synthesis of N-CNTs/β-CD polymer composite

A 1% (w/w) N-CNT/ β-CD polymer nanocomposite was synthesized by first dispersing 0.04 g of *f*N-CNTs in 4 ml of dimethyformamide (DMF) by sonication. This solution mixture was then added to a round bottom flask containing β-CD in 40 ml DMF. A linker, hexamethylene diisocyanate (HMDI) (4 ml) was then added drop-wise to this mixture. The resulting mixture was then heated at 70 ºC for 24 h under inert conditions by purging $N_{2.}$ After 24 h, the resulting polymer composite was washed in acetone and left to dry overnight in a fume hood [3]. The composite was then characterized using Fourier Transform-Infrared Spectroscopy (FT-IR), Thermal Gravimetric Analysis (TGA), Brunauer Emmett and Teller (BET) and Scanning Electron Microscopy (SEM).

3.4 Microwave-assisted synthesis of N-CNT/β-CD polymer composite

The *f*N-CNTs (0.04 g, 1% of the *f*N-CNTs based on the mass of the polymer) were dispersed in 4 ml DMF and added to a beaker containing 4g β-CD (99 % polymer loading) in 40 ml DMF. HMDI (4 ml) was then added drop wise to this mixture. The mixture was then carefully transferred into a reaction vessel and placed in an industrial microwave (Anton Paar, Multiwave Synthon 3000). Nitrogen gas was then purged into the vessels for 3 min to provide inert reaction conditions. The vessels were then heated for 15, 10, and 30 min at 600 W irradiation power while stirring. Similar composites were also synthesized in the

microwave while varying the power parameter, 400 W and 800 W. The resulting nanocomposites polymer were washed in acetone and left to dry overnight. The materials were then characterized using FT-IR, TGA, BET and SEM.

3.5 Removal of *p*-nitrophenol

The N-CNT/β-CD (0.60 g) nanocomposites polymers prepared by the conventional and microwave-assisted methods were packed in empty Solid-Phase-Extraction (SPE) cartridges with polyethylene frits on both ends of the polymer to maintain good polymer packing during percolation. Water samples spiked with PNP (30 ml, 10 $\mu g \cdot l^{-1}$) were then passed through the polymers at a flow rate of about 3 ml to 5 $ml \cdot min^{-1}$. As a control, a cartridge containing only the two polyethylene frits was used to check if their polymeric nature will contribute to the absorption of the pollutant. The resultant filtrates were then analysed using ultraviolet (UV-Vis) spectroscopy.

3.6 Removal of trichloroethylene (TCE) and bisphenol A

TCE and bisphenol A samples were prepared by spiking a known amount of the pollutant in deionized water. Solid phase extraction was then used to test for the removal of TCE by the synthesized polymers. Polymers were first packed in Supelclean™ ENVI™ 18 SPE material in glass tubes with PTFE frits and the water samples were percolated through. Resulting filtrates were preconcentrated and quantified using gas chromatography-mass spectrometry (GC/MS).

3.7 Microwave synthesise of Ag/N-CNTs

The dispersion of Ag on the N-CNTs (Ag/N-CNTs) was achieved by the microwave heating of ethylene glycol (EG) solutions of $AgNO_3$ salt. Typically 1.0 mL of an aqueous solution of 0.5 M $AgNO_3$ (Sigma-Aldrich Reagent) was mixed with 25 mL of EG (Sigma-Aldrich Reagent), 0.4 ml of 0.8 M KOH in a 100 ml beaker. N-CNTs (1 g) were uniformly dispersed in the mixed solution by ultrasound. The beaker contents were then poured into a reaction vessel and placed in an industrial microwave (Anton Paar, multiwave 3000) and heated for

60 s under a microwave power of 700 W. The resulting suspension was centrifuged and the residue was washed with acetone. The solid black product recovered was then dried at 100 ºC over night in an oven. The percentage loading of Ag on the N-CNTs was quantified using TGA by burning the materials in air at 850 °C to remove the carbon, which decomposed at 550 °C.

3.8 Microwave synthesis of Ag/N-CNTs/β-CD

Prior to preparation of Ag/N-CNT/β-CD polymer nanocomposites, the Ag/N-CNT nanocomposites (1.0 g) were sonicated in ultrapure distilled water for 12 h in a beaker. Small portions of the water were drawn at 30 min intervals and analysed using Inductively Coupled Plasma – Optical Emission Spectroscopy (ICP-OES). The samples were found to contain no Ag. TEM analysis revealed that the AgNPs were still bound on the surface of the N-CNTs intactly.

A conventional synthesis procedure used by Salipira *et al* was adopted for this work [3] . To synthesise the nanocomposites in a microwave, 0.04g of the functionalized Ag/N-CNTs (1% loading) were dispersed in 5 ml DMF and added to a beaker containing 4g β-CD (99 % polymer loading) in 50 ml DMF. HMDI (4 ml) was then added drop wise to this mixture. The mixture was then carefully transferred into two reaction vessels, purged with nitrogen gas, sealed and placed in an industrial microwave (Anton Paar, Multiwave 3000). The vessels were then heated for 10 min at 600 W while stirring. The resulting nanocomposite polymers were washed in acetone and dried under vacuum. The polymers were then tested for their efficiency in destructing *E. coli* in spiked water samples and real water samples.

3.9 Antibacterial testing

A spiked water sample was first prepared by adding *E. coli* bacteria in water and the concentration was 1 x 10^5cfus/ml (colony forming units) prior to treatment. Ag/N-CNTs and Ag/N-CNTs/ β-CD polymer composites were then placed in 10 ml of culture (for 24 h) and spotted on HiChrome plates with standard concentration of cells sample. After 24 h, counts were taken. All work was carried in triplicate to validate the outcomes. The plating was done in duplicate and 100 µl of water sample was spread on the plates.

CHAPTER 4: CHARACTERIZATION AND APPLICATION OF *f*N-CNTs/β-CD POLYMER NANOCOMPOSITES

4.1 Characterization of N-CNTs

4.1.1 TEM

N-CNTs were successfully synthesized over a 10 wt.% Fe-Co/$CaCO_3$ catalyst in a CVD furnace. The N-CNTs were collected as a black powder in a quartz crucible. TEM images of the N-CNTs before and after purification are presented in Fig. 14. The N-CNTs have open tips suggesting that their mechanism of growth was via the root growth mechanism [16]; hence the purified materials have no residual catalyst. The successful doping with nitrogen was also confirmed by the presence of bamboo compartment within the inner walls of the N-CNTs [16]. A large percentage of the N-CNTs have an outer diameter ranging between 30 and 40 nm as shown in Fig. 15.

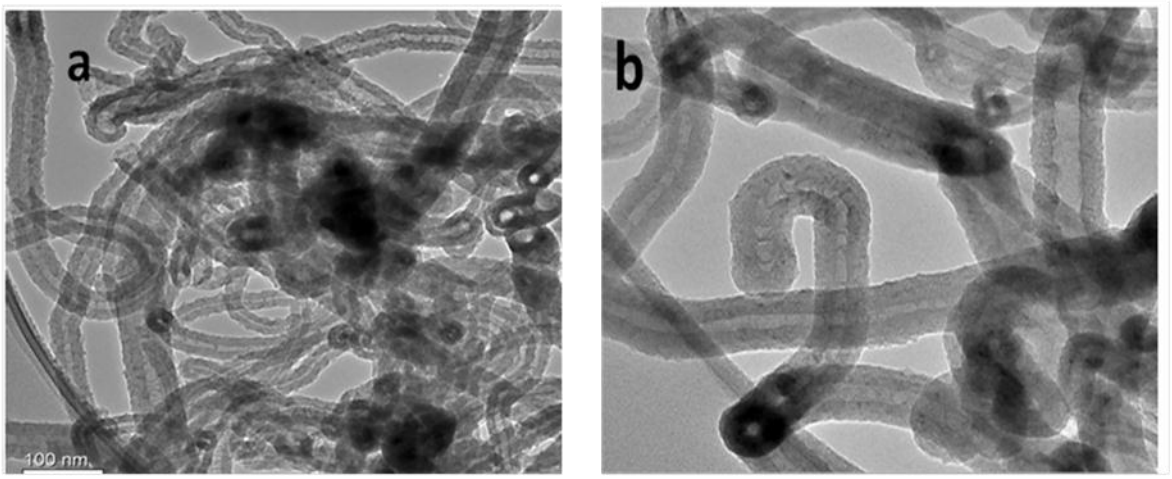

Fig. 14: TEM images of the synthesized N-CNTs before (a) and after purification (b).

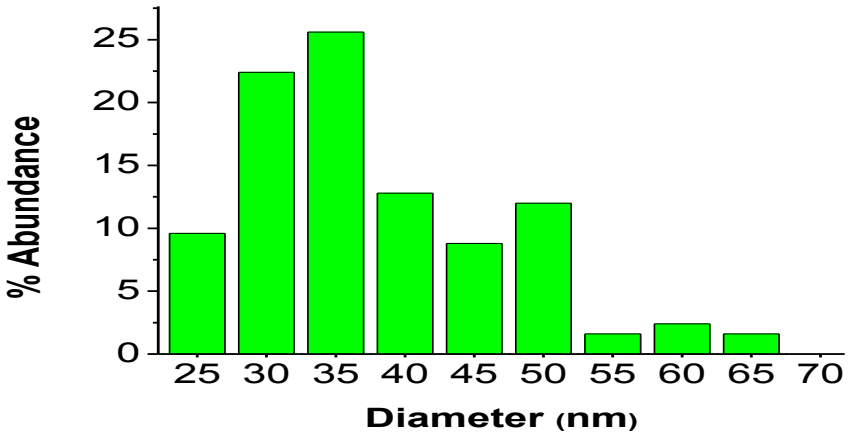

Fig. 15: Outer diameter distribution of the purified N-CNTs.

4.1.2 CN and XPS analysis

Quantification of the N content in the N-CNTs was achieved via the carbon and nitrogen (C% and N%) analysis method using a Carlo Erba NA 1500 C/N/S analyser, which uses GC (gas chromatographic) separation of the gases produced on total combustion of the sample. The average percentage of N in the N-CNTs was 2.5%. The N doping level and the types of N-moieties in the N-CNTs was also confirmed by X-ray photoelectron spectroscopy (XPS). Previous work has shown that the N can be incorporated into the CNT lattice in different bonding configurations; namely, (i) pyridine-like N: where the N atom is sp^2 hybridized, bonding to two C atoms, (ii) pyrrole-like N: where the N is sp^3 hybridized in a five-membered ring, (iii) quaternary/graphitic/substitutional N: where a graphitic carbon atom is substituted by a N atom in the graphitic sheet and (iv) pyridinic oxides: which are attributed to oxidized nitrogen on the graphite layers (Fig. 16) [104].

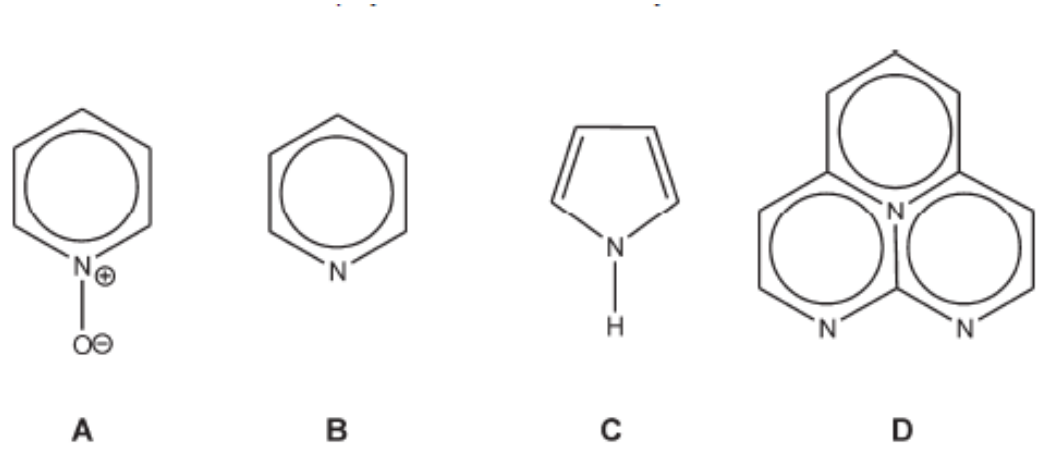

Fig. 16: Types of nitrogen moieties that can be incorporated into graphitic carbon: (A) oxidized pyridinic, (B) pyridinic, (C) pyrrolic, (D) quaternary [105].

Fig. 17a shows a high-resolution N 1s XPS spectrum of the N-CNTs, which shows the presence of nitrogen-based species on the N-CNT structure. The N 1s peak can be deconvoluted into three peaks: pyridinic oxides (NO_x at 405 eV), quaternary nitrogen (N_Q at 401 eV) and pyridinic nitrogen (N_P at 398 eV). The N 1s spectra revealed that N atoms in the outer layer mainly exist as pyridinic oxides while quaternary and pyridinic nitrogen are less abundant. No pyrrolic nitrogen peak was observed on the XPS spectra. However we believe that these N species could be present in the inner walls of the tubes and they could be responsible for the formation of the curvatures (bamboo-like structures) in the inner walls of the N-CNTs (Fig. 17b). Indeed, the formation of curvature e.g. in graphitic carbon spheres occurs as a result of a pentagonal ring in the graphite structure [106-108], which assumes the same structure observed with pyrrolic nitrogen.

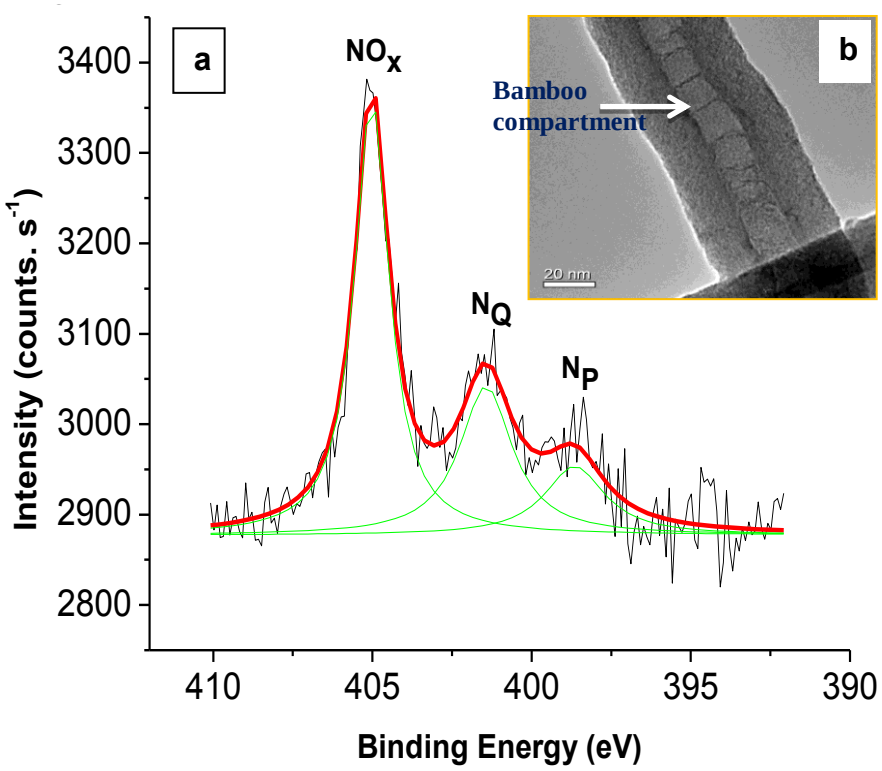

Fig. 17: XPS spectrum showing a deconvoluted N 1s spectrum of the functionalized N-CNTs.

4.1.3 *TG analysis (TGA)*

TGA was employed to investigate the thermal stability and purity of the N-CNTs. Fig. 3 shows the TGA profiles for the as-synthesised N-CNTs (with catalyst) and the functionalized N-CNTs (*f*N-CNTs) at different acid treatment times (i.e. 2, 4, 6 and 8 h) heated in air. A complete removal of the catalyst after acid treatment was observed as shown by the absence of the catalyst decomposition peak at 700 ºC. The N-CNTs were stable up to 600 ºC where all the carbon decomposed. Increasing the acid treatment time to 8 h did not compromise the thermal stability of the N-CNTs. An acid treatment time of 8 h was sufficient to remove the residual catalyst and the catalyst support from the N-CNTs. The method to synthesize the N-CNTs is still being optimized in our research group.

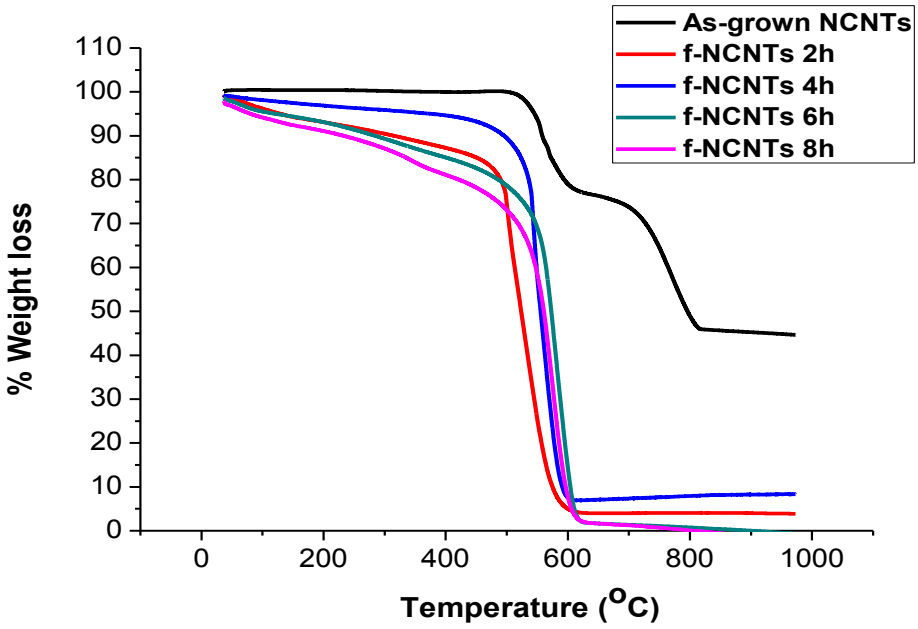

Fig. 18: TGA profiles of the as-synthesized N-CNTs and *f*N-CNTs refluxed in HNO_3 at different times.

4.1.4 FT-IR analysis and Zeta potential analysis

FT-IR analysis confirmed the formation of acidic groups (-COOH, -OH) on the surface of the N-CNTs (Fig. 19) after treatment with nitric acid. The formation of these acid functional groups was achieved for all the acid treatment times employed (i.e 2, 4, 6, 8 h), however at different degrees. The peak appearing at ~1717 cm^{-1} was ascribed to the C=O stretching vibration of carboxyl or carbonyl groups while the peak at 1248 cm^{-1} corresponds to C–O stretching and O–H bending vibrations [3, 109]. These peaks were not observed on the as-grown N-CNTs suggesting that indeed the N-CNTs were successfully functionalized.

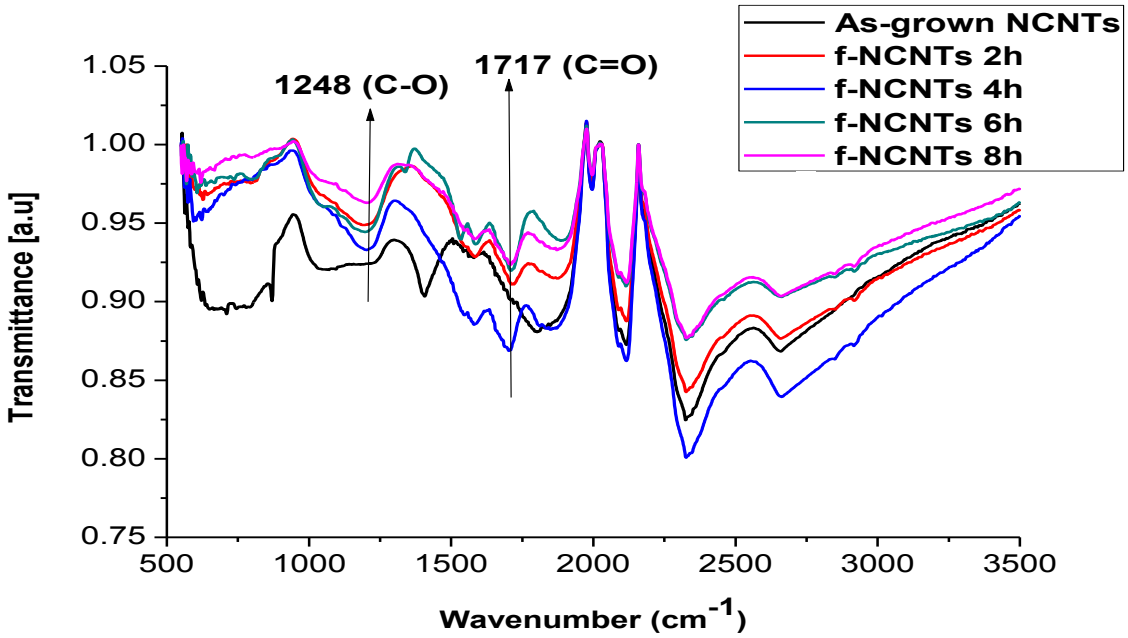

Fig. 19: FT-IR spectra of the as-synthesized and *f*N-CNTs refluxed in HNO_3 at different times.

The determination of the zeta potential of the *f*N-CNTs was used to quantify the presence of oxygen surface groups. The presence of acidic groups causes the carbon surface to be more hydrophilic, increasing the negative surface charge density and decreasing the pH of the point of zero charge (PZC) [109, 110]. Fig. 20 shows the plots of zeta potential of the as-grown N-CNTs and *f*N-CNTs as a function of pH. The PZC of the as-synthesized N-CNTs occurs at a pH of 6.5. At pH < 6.5, the surface of the N-CNTs is positively charged and at pH > 6.5 the surface is negatively charged. After acid treatment, the PZC shifts to lower pH values due to the introduction of surface oxygen groups. The *f*N-CNT-2h has a pH_{pzc} ~ 2.8. As the acid treatment time is increased, the PZC values shift further to even lower pH. Indeed, the *f*N-CNTs-4h, *f*N-CNTs-6h and *f*N-CNTs-8h all have values below pH 2. These results suggest that acidic functional groups are formed on the N-CNT surface and their concentration increases with acid treatment time. The high degree of functionalization observed was required for this study to ensure good dispersion of the *f*N-CNTs in the polymer matrix.

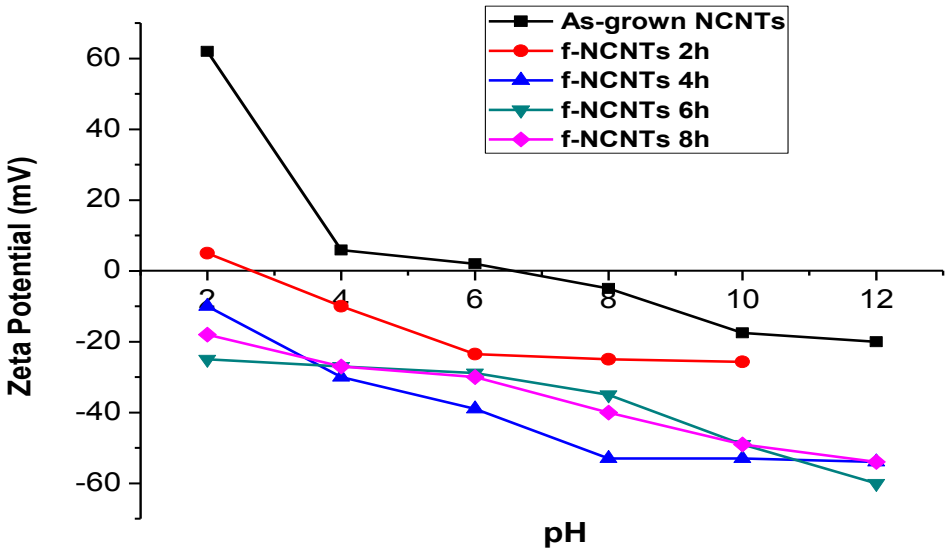

Fig. 20: Zeta potential measurements of the as-synthesized and *f* N-CNTs as a function of pH.

4.1.5 Surface area analysis of the N-CNTs

Table 4 presents the Branauer-Emmet-Teller (BET) surface areas, pore volumes and average pore sizes of the as-synthesized and *f*N-CNTs. The results indicate that the *f*N-CNTs possess higher surface areas. This is attributed to the roughness and defects that are created during acid treatment process [109, 111]. The high surface area generally results to a good dispersion of metal nanoparticles on the surface of the CNTs. The roughness provides suitable docking stations for the particles and reduces the chances of agglomeration of the metal nanoparticles. Thus these N-CNTs were suitable for our study.

Table 4: BET surface areas of the as-synthesized and *f*N-CNTs used to prepare polymer composites with β-CDs.

Sample name	BET surface area (m^2/g)	Pore volume (cm^3/g)	Average Pore Size (nm)
As-synthesized N-CNTs	25	0.10	29.6
*f*N-CNTs	52	0.17	15.6

4.2 Characterization of *f*N-CNTs/β-CD nanocomposite materials

4.2.1 FT-IR analysis

FT-IR analysis was performed in order to confirm successful polymerization of the *f*N-CNTs with the β-CDs using two different synthesis methods. The absence of the isocyanate peak (NCO) of the linker (at 2250 cm^{-1}) confirmed that polymerization between all the components to form the *f*N-CNTs/β-CD polymer nanocomposite had taken place (Fig. 21). FT-IR spectra of the resulting polymers containing 1% (w/w) *f*N-CNTs prepared using microwave-induced synthesis (M-10 min, M-15 min and M-30 min; M = microwave heating time) and polymer nanocomposites prepared by the conventional method are shown in Fig. 21. The presence of some of the functional groups O-H (3390 cm^{-1}), C=C (1631 cm^{-1}), C-H (2938 cm^{-1}) and C-O (1034 cm^{-1}) which were inherited from the *f*N-CNTs also confirmed the presence of *f*N-CNTs in the prepared composite. Due to the efficient homogenous heating achieved through microwave irradiation, complete polymerization was attained at very short period of time (i.e. 10 min) when compared to the conventional method which takes 24 h [3, 15, 20, 79, 112]. All the synthesised polymers were found to be insoluble in water, which is a desirable characteristic for their intended application in water purification.

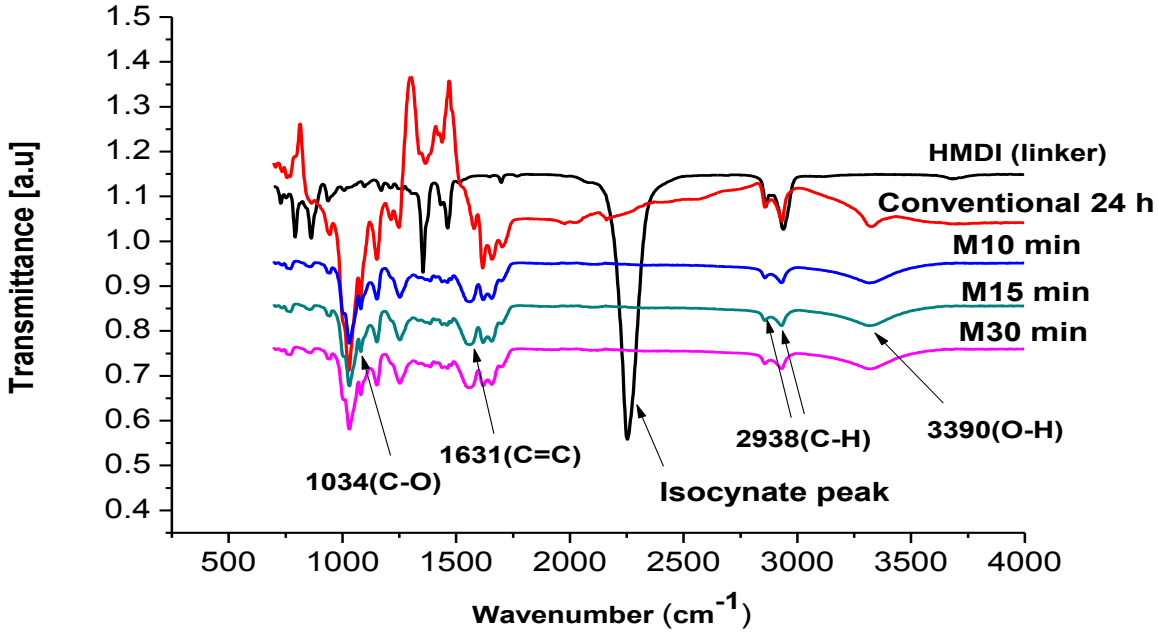

Fig. 21: FTIR spectra of the polymer nanocomposites showing the absence of the isocyanate peak. The absence of the peak suggests complete polymerization.

Similar polymer nanocomposites were also synthesized at different powers of 400 W, 600 W and 800 W at 10 min irradiation which was found above (Fig. 21) to be sufficient to attain complete polymerization. The FT-IR spectra, Fig. 22 shows that complete polymerization was attained for all the different powers thus suggesting that these materials can also be synthesized at lower powers, e.g. 400 W.

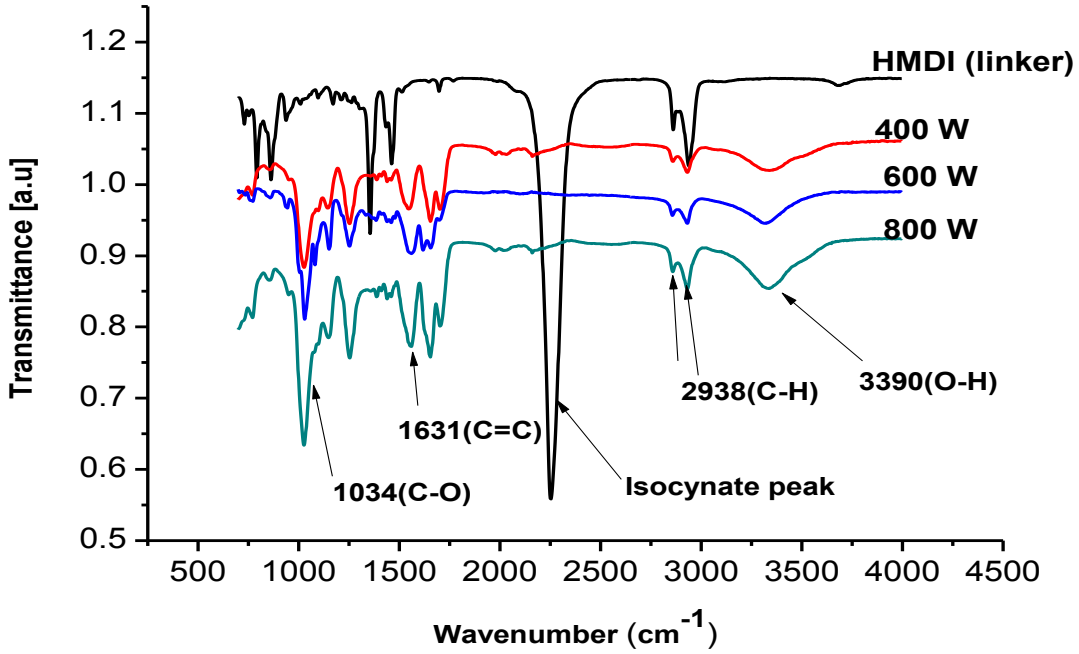

Fig. 22: FTIR spectra of the polymer nanocomposites synthesized at different microwave irradiation powers of 400 W, 600 W and 800 W for 10 min.

4.2.2 TG analysis (TGA)

TGA was performed to investigate the thermal stability of the polymers. The decomposition peak for the native β-CD polymer occurs at 340 ºC as shown on the derivative weight profiles (Fig. 23). After incorporating the *f*N-CNTs via the conventional method, there is a significant reduction in the decomposition of the polymer at that temperature. This suggests that adding the *f*N-CNTs improves the thermal stability of the polymer due to the strong bond formed between the *f*N-CNTs and the β-CDs. A slight shift in the decomposition of the nanocomposite polymers prepared by the microwave was observed (indicated by dotted line). This slight decrease in thermal performance is not expected to have negative effects on the application of these polymers in water purification since temperatures used are low (normally

room temperature). The TGA profile also indicates that the native β-CDs had a lot of moisture which was lost at around 100 ^{o}C.

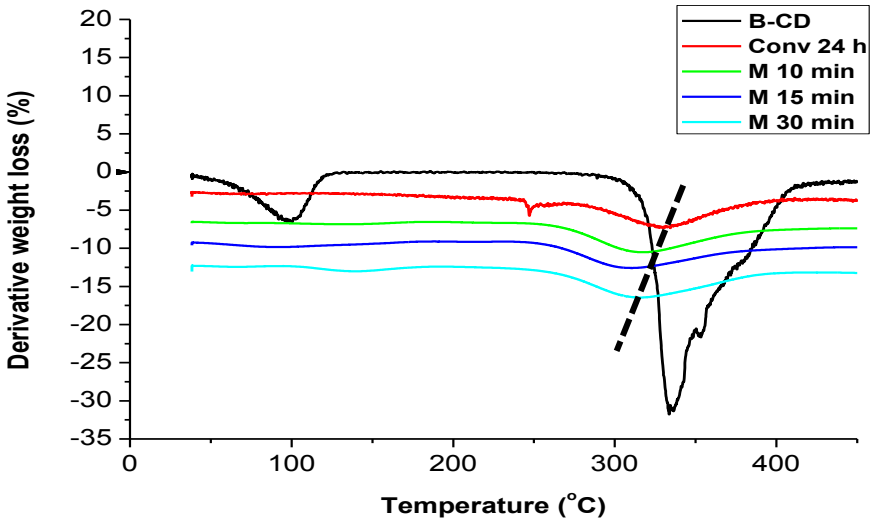

Fig. 23: Derivative weight % profiles for β-CD and *f*N-CNTs/β-CD synthesized via the conventional and microwave-induced methods.

The effect of synthesis power on the thermal stability of the resulting polymer composite was also studied using TG analysis. The spectra, Fig. 24, indicates that varying the power does not significantly compromise the thermal stability of the polymers but rather improve its stability as observed from the decrease in the intensity of the β-CD decomposition peaks. The 600 W slightly shifted the stability to a lower temperature as compared to the lower (400 W) and higher (800 W) powers. No specific trend can therefore be deduced with respect to power on the thermal stability.

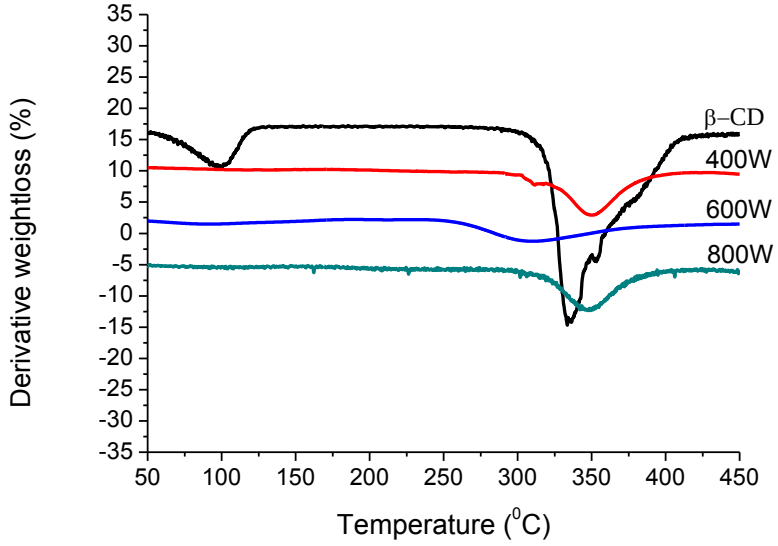

Fig. 24: Derivative weight % profiles for β-CD and *f*N-CNTs/β-CD synthesized via the microwave-induced method at different irradiation powers.

4.2.3 Structural morphology of the polymer nanocomposites

Fig. 25 shows SEM images of the polymer nanocomposites synthesized by the conventional and microwave-induced methods. The images indicate the differences in the microstructure of the polymers. The polymers synthesized by the microwave method were less densely packed and seemed to have a higher surface area, which is necessary to allow for efficient contact between the polymer and the pollutant. The conventional polymers display a more densely packed morphology. Previous studies [3] on *f*N-CNTs/β-CD synthesised by conventional method reports a composite that has a spongy appearance after incorporating 1% *f*N-CNTs into the β-CD which is different from the conventional polymers reported in this study. This may be attributed to the inconsistency that arises when convectional synthesis is employed since it creates different thermal gradients within the reaction vessels [113]. Reaction vessels act as intermediary for energy transfer from the heating mantle to the bulk solvent and eventually to the precursor molecules. This can cause sharp thermal gradients, non-uniform and inefficient conditions in the vessels [113, 114]. This difference in morphology did not however affect the performance of these polymers as they have shown to be effective in their removal of PNP from spiked water samples as shown in the UV-Vis spectra (Fig. 27). Compared to the polymers synthesized in a microwave, which were

powdery and soft, the polymers synthesised by the conventional method were granular, hard and coarse-like.

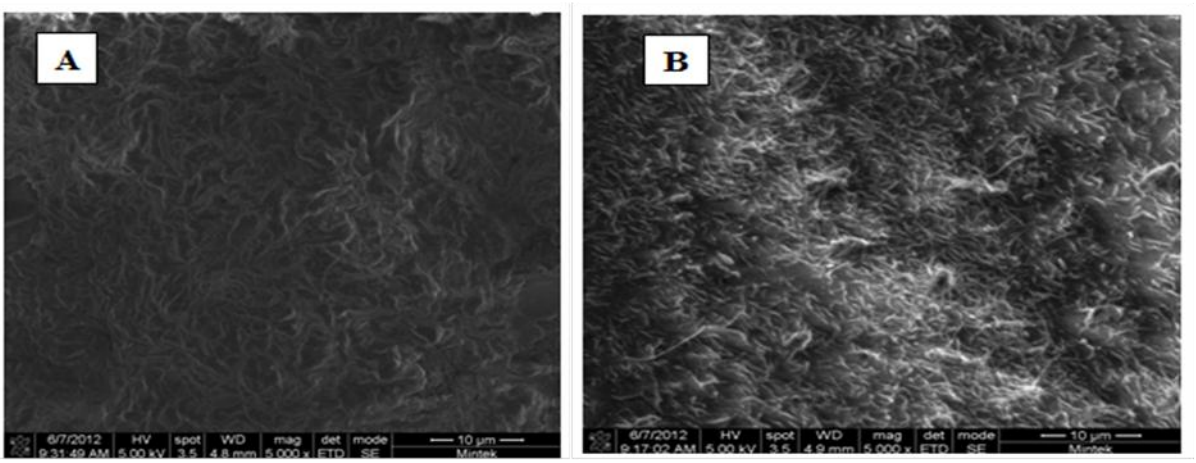

Fig. 25: SEM images of the *f*N-CNTs/β-CD polymer nanocomposites synthesized by the conventional method (a) and microwave method (b).

The effect of microwave irradiation power on the polymer composite morphology was also studied using SEM. Fig. 26 shows the different morphologies of polymers synthesized at (a) 400 W, (b) 600 W and (c) 800 W irradiation power.

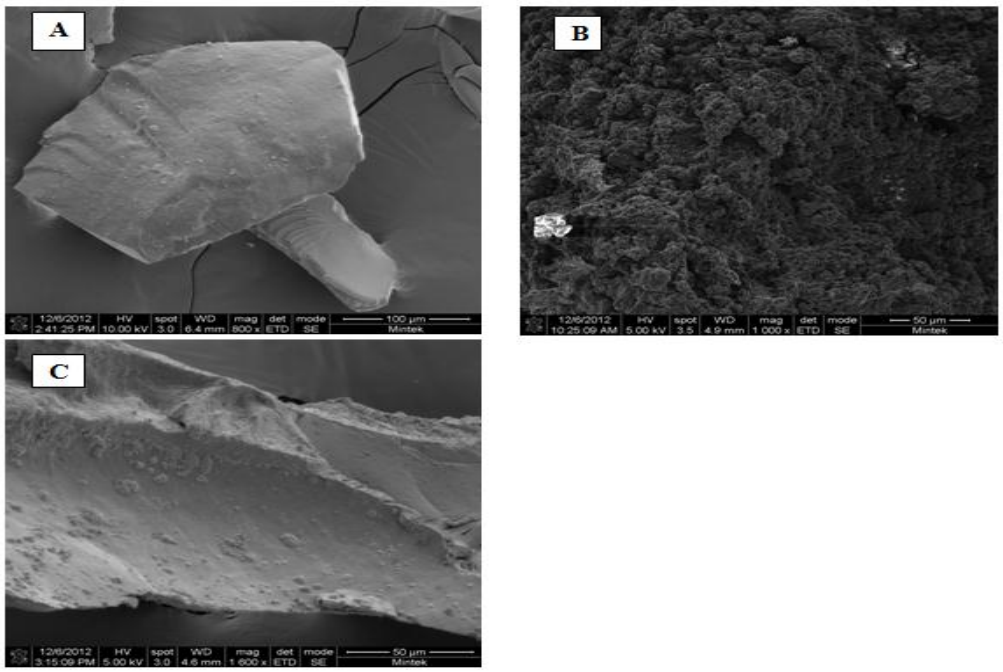

Fig. 26: SEM images of the *f*N-CNTs/β-CD polymer nanocomposites synthesized by microwave-induced method at different irradiation powers: (a) 400 W, (b) 600 W, (c) 800 W.

As can be seen from the micrographs (Fig. 26), microwave irradiation power has some influence on the morphology of the polymer composites. The 400 W and 800 W powers produced composites that are dense and smooth as opposed to the 600 W synthesized composite that displayed a porous and rough surface. This suggests that the amount of microwave energy used during microwave synthesis must be carefully selected in order to maintain the porous nature of the polymers.

*4.2.4 Surface area of f*N-CNTs/β-CD *polymer nanocomposites*

Table 5 shows the surface area of *f*N-CNTs/β-CD polymer nanocomposites synthesized by conventional and microwave-induced method (at different powers). The conventional method yielded polymers with lower surface area as compared to the microwave synthesized polymers. This is in agreement with the SEM micrographs reported above (Fig. 26). By varying the microwave irradiation power, the surface area of the polymers is significantly altered. A lower power (400 W) yielded a lower surface area compared to the higher powers and 600 W was observed to give the highest surface area, 1.5 m^2/g.

Table 5: Surface area of conventional and microwave synthesized *f*N-CNTs/β-CD polymer nanocomposites

Sample name	**BET surface area (m^2/g)**	**Pore volume (cm^3/g)**
Conventional	0.40	0.0024
Microwave (400 W)	0.59	0.0013
Microwave (600W)	1.5	0.012
Microwave (800W)	0.98	0.0029

The effect of irradiation time on the surface area was also studied using BET. The polymers were synthesized at an optimum power of 600 W. A synthesis time of 10 min gave the highest surface area, 1.5 m^2/g. Increasing the synthesis time led to a decrease in the surface area of the polymers (Table 6).

Table 6: Surface area of *f*N-CNTs/β-CD polymer nanocomposites synthesized at different synthesis times

Sample name	BET surface area (m^2/g)	Pore volume (cm^3/g)
10 minutes	1.5	0.0017
15 minutes	0.59	0.0014
30 minutes	0.58	0.0015

4.3 UV-VIS analysis for the removal *p*-nitrophenol

The absorption of a widely known priority organic pollutant (*p*-nitrophenol) was studied using the *f*N-CNTs/β-CD polymer nanocomposites synthesized *via* the conventional and microwave methods (Fig. 27). Before extraction, the spiked water sample was analysed in order to get an initial reading of the absorbance and use it as a reference to trace the efficiency of the polymers. The frits used in the SPE extraction set up to allow for uniform and consistent packing of the polymer were made of polyethylene. As a control, spiked water samples were also percolated through an SPE cartridge without the nanocomposites polymers to establish whether the frits had some effect in the retention of the pollutant.

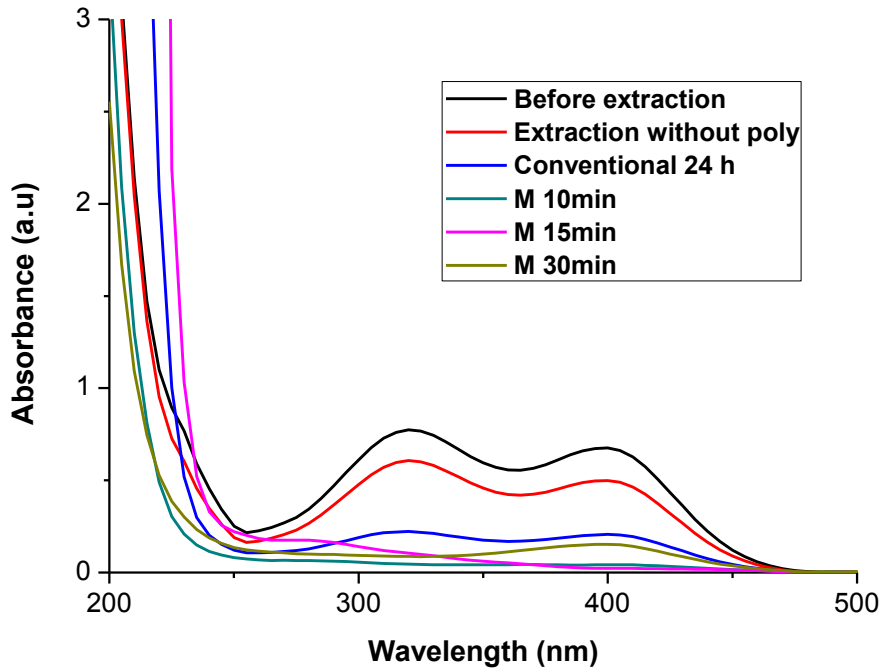

Fig. 27: UV-Vis Absorbance spectra for *f*N-CNTs/β-CD polymer composite synthesized *via* the conventional and microwave methods.

Fig. 27 shows that after percolating the solution through the frits, there was some degree of absorption of the PNP molecule by these frits but it was not a significant absorption. The polymers were then packed uniformly in the cartridges and the sample was percolated. After percolating the solution through the polymers, there was ~ 98% (conventional method) – 100 % (microwave) removal of the PNP from the water samples as shown in Fig. 27. The colour changes for the spiked water samples before (left) and after (right) percolation are indicated in Fig. 28. After percolation, the samples changed colour from yellow to clear. It was observed that 10 min of microwave irradiation time was sufficient for the synthesis of the *f*N-CNTs/β-CD polymer nanocomposites that were capable of completely removing the organic pollutant from water. Indeed these polymers have been shown in our earlier studies to be very efficient in removing organics [15]. However, a much greener and shorter method is presented here.

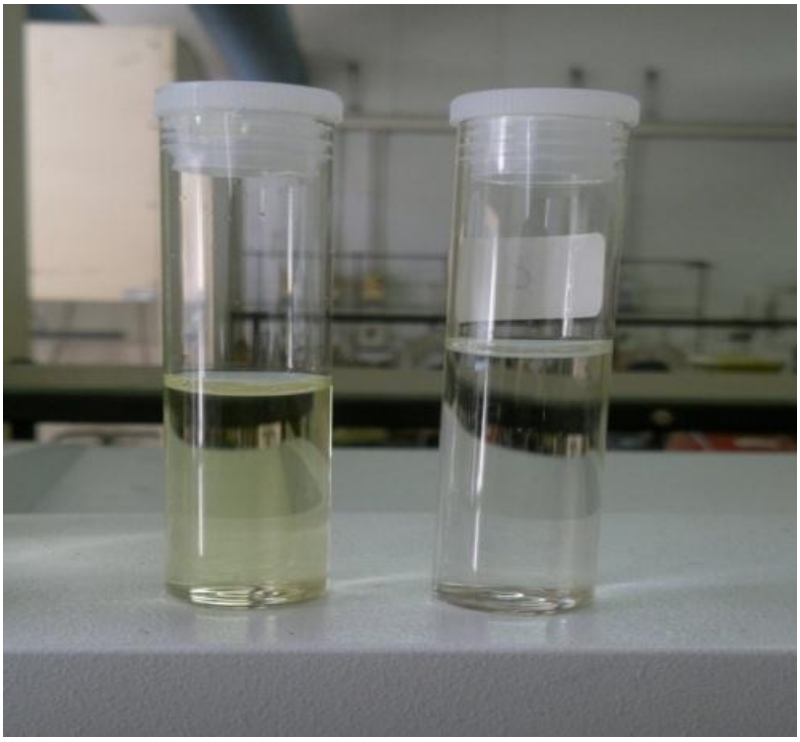

Fig. 28: Colour changes of spiked water samples before (left) and after (right) percolation through polymer matrix.

CHAPTER 5: CHARACTERIZATION AND APPLICATION OF Ag/*f*N-CNTs/β-CD POLYMER NANOCOMPOSITES*

5.1 Characterisation of Ag/*f*N-CNTs

5.1.1 TEM and EDS analysis

The effect of using microwave and a conventional wet impregnation method on the synthesis of Ag/*f*N-CNTs was studied to ascertain the effect of using microwaves. Fig. 29 shows TEM images of Ag/*f*N-CNTs synthesized using both methods. A uniform dispersion of the Ag NPs on the N-CNTs can be observed (Fig. 29a). Poor dispersion of the Ag NPs was observed when the nanocomposites were prepared using the wet impregnation method (Fig. 29b); the NPs were agglomerated in some regions (region 1) and not present in some regions of the N-CNTs (region 2).

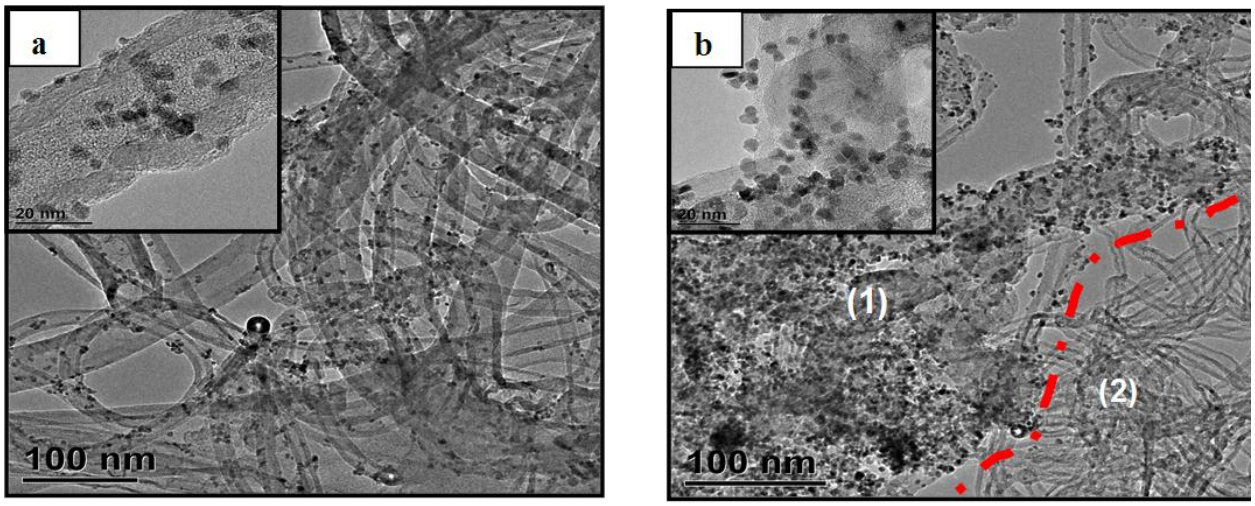

Fig. 29: (a) A TEM and high magnification image (inset) of Ag/N-CNTs prepared under microwave irradiation; (b) a TEM and high magnification image (inset) of Ag/N-CNTs prepared using the wet impregnation method. The dark sports are the Ag NPs.

---

*A part of this work has been published in Nanoscience and Nanotechnology Letters [115].

A large percentage of the Ag NPs had diameters of 2.5 nm and 3.5 nm as presented in Fig. 30. Small particle sizes of Ag NPs exhibit high surface area which allows for efficient interaction between the particles and bacterial species during water disinfection [2]. EDS confirmed the successful dispersion of Ag NPs on the surface of the *f*N-CNTs, Fig. 31.

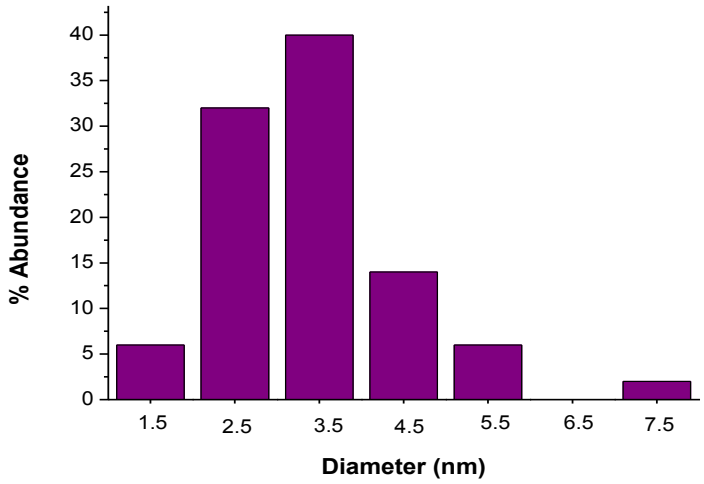

Fig. 30: Diameter distribution of the Ag nanoparticles.

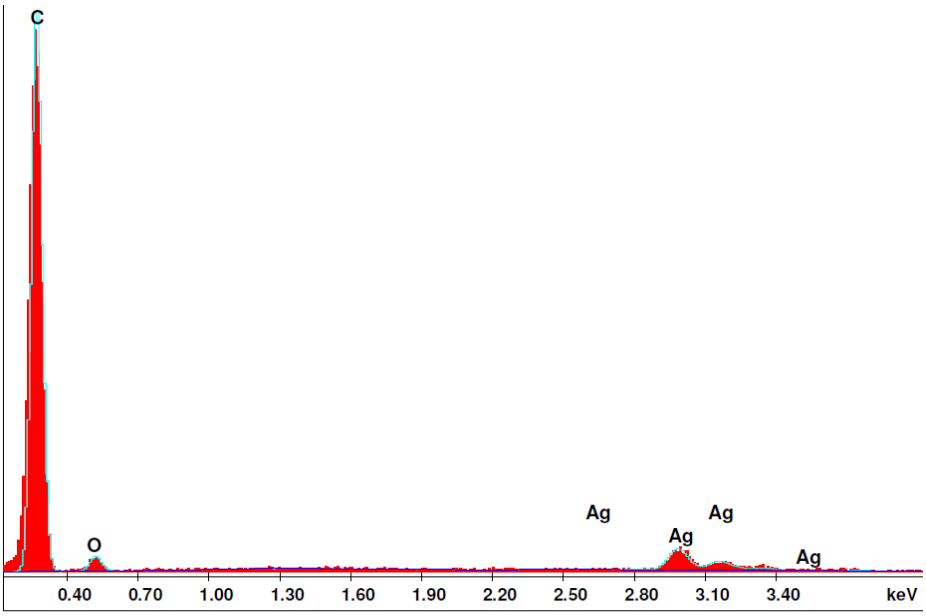

Fig. 31: EDS confirming the presence of Ag nanoparticles in 20 wt. % Ag/*f*N-CNTs.

5.1.2 TG analysis of Ag/fN-CNTs

TG analysis was used to investigate the thermal stability and to establish whether the loading Ag NPs on the N-CNTs was successful. The TGA profile showed that dispersing the Ag nanoparticles slightly shifted the thermal stability of the N-CNTs to a lower temperature (450 ^{o}C), Fig. 32. The residual weight loss (%) between the N-CNTs and Ag/*f*N-CNTs indicates the percentage loading of Ag. The % loading is analogous to EDS data which showed only the presence of Ag metals in the sample. The % loading of Ag was found to be is ~ 18% which is slightly different from the theoretical loading of 20% Ag. The difference in percentage loading could be ascribed to errors during sample preparation. Also while good dispersion was observed, it may not have been 100% uniform hence the variation in the portions of the sample that was analysed.

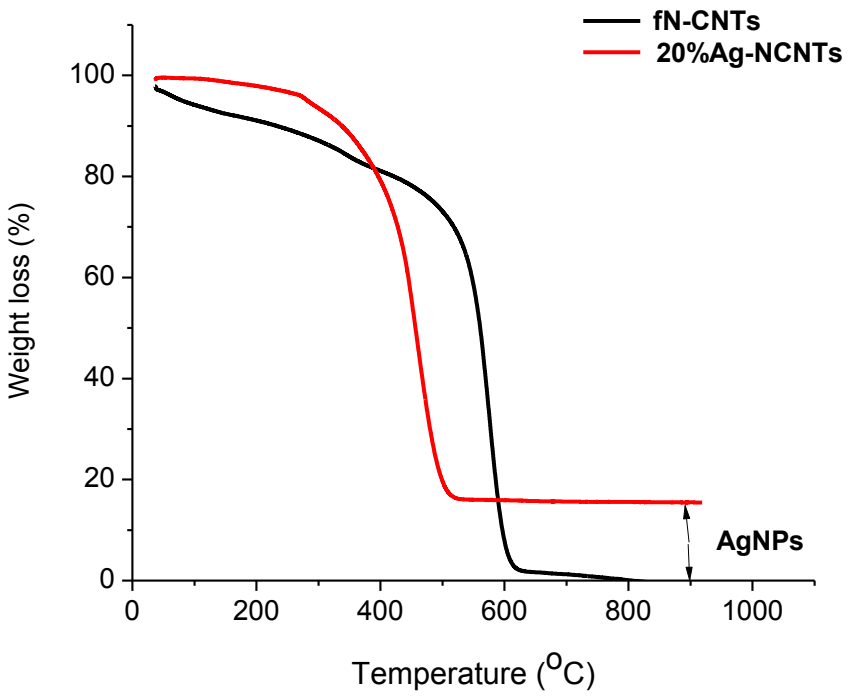

Fig. 32: Weight loss profile for *f*N-CNTs and Ag-NCNTs.

5.2 Characterization of Ag/*f*N-CNTs/ β-CD nanocomposites

5.2.1 FT-IR analysis

A 20 wt.% Ag/*f*N-CNTs/β-CD composite was synthesized using the optimum microwave conditions; 600 W and 10 min irradiation time. Successful synthesis of the polymer composite was confirmed by the absence of the isocyanate peak (NCO) of the linker (at 2250 cm^{-1}) (Fig. 33). The presence of functional groups O-H (3390 cm^{-1}), C=C (1631 cm^{-1}), C-H (2938 cm^{-1}) and C-O (1034 cm^{-1}) which were inherited from the *f*N-CNTs also confirmed that polymerization had occurred.

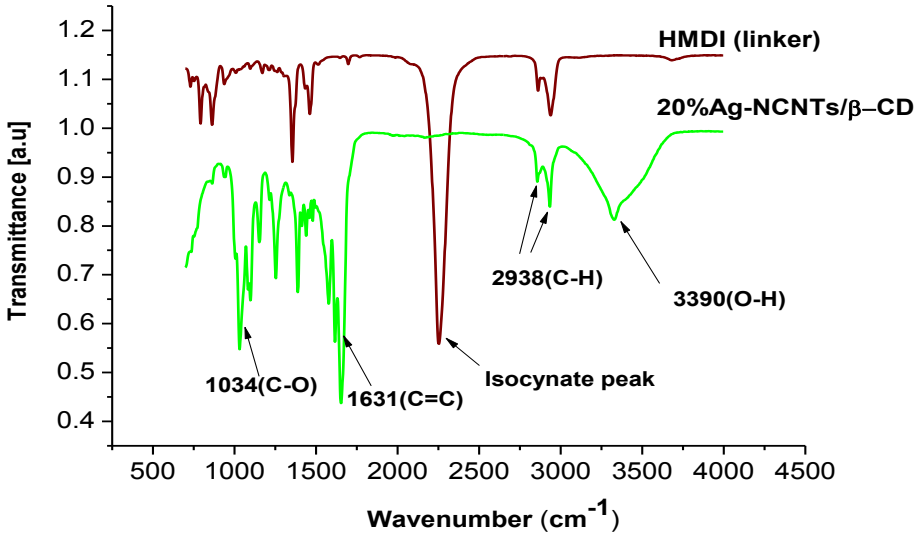

Fig. 33: FTIR spectra confirming the successful synthesis of 20 wt.% Ag/NCNTs/β-CD polymer nanocomposite.

5.2.2 TG analysis

TG analysis was used to study the influence of Ag loading on the thermal stability of β-CD. Fig. 34 shows that both *f*N-CNTs/β-CD and 20 wt.% Ag/*f*N-CNTs/β-CD polymer composites resulted in a slight decrease in the decomposition temperature of β-CD from 340 °C to 300

°C. The shift is due to the irradiation power, 600 W, which was used to synthesize these polymers as explained in section 4.2.2. The addition of Ag on N-CNTs therefore did not affect the thermal stability of β-CD.

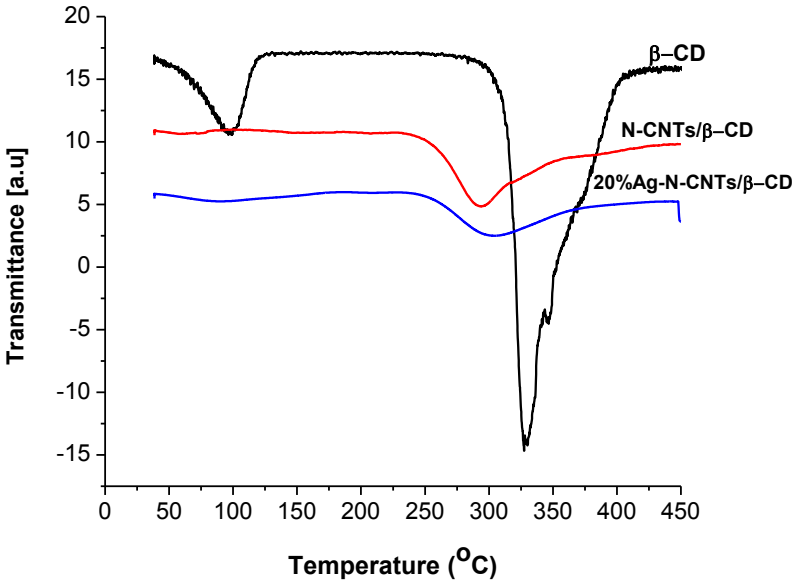

Fig. 34: Derivative weight loss profile for native β-CD, *f*N-CNTs/β-CD and 20 wt.% Ag/*f*N-CNTs/β-CD polymer nanocomposites.

5.2.3 *Structural morphology and EDS analysis of 20 wt.% Ag/N-CNTs/β-CD polymer nanocomposites*

The 20 wt.% Ag/*f*N-CNTs/β-CD polymer nanocomposites displayed a very porous and spongy morphology as observed on the SEM micrograph (Fig. 35). This morphology is consistent with similar polymer nanocomposites synthesized by Lukhele *et al* using conventional methods [116]. A porous and spongy morphology is associated with higher surface area which is critical for improved interaction between the polymers and organic pollutants and bacteria.

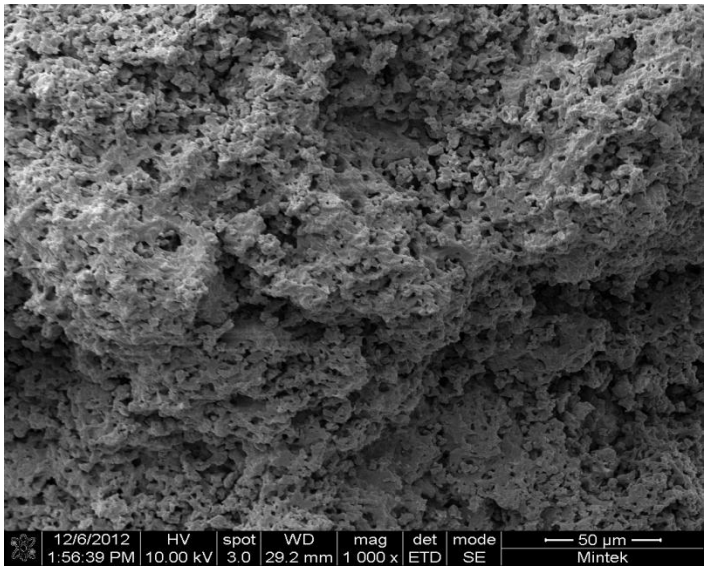

Fig. 35: SEM micrograph of 20wt%Ag/*f*N-CNTs/β-CD polymer nanocomposites.

During the synthesis of the 3 component nanocomposite, 20 wt.% Ag/*f*N-CNTs/β-CD, the possibility of Ag nanoparticles being leached out from the system cannot be ruled out. EDS analysis was performed on the 20 wt.% Ag/*f*N-CNTs/β-CD polymer nanocomposite to confirm the presence of the Ag nanoparticles. The EDS spectrum confirms the presence of Ag nanoparticles embedded within the polymer, Fig. 36. The Au peak that appears in the spectrum was due to the gold coating that was done on the sample prior to analysis to prevent it from charging and burning out.

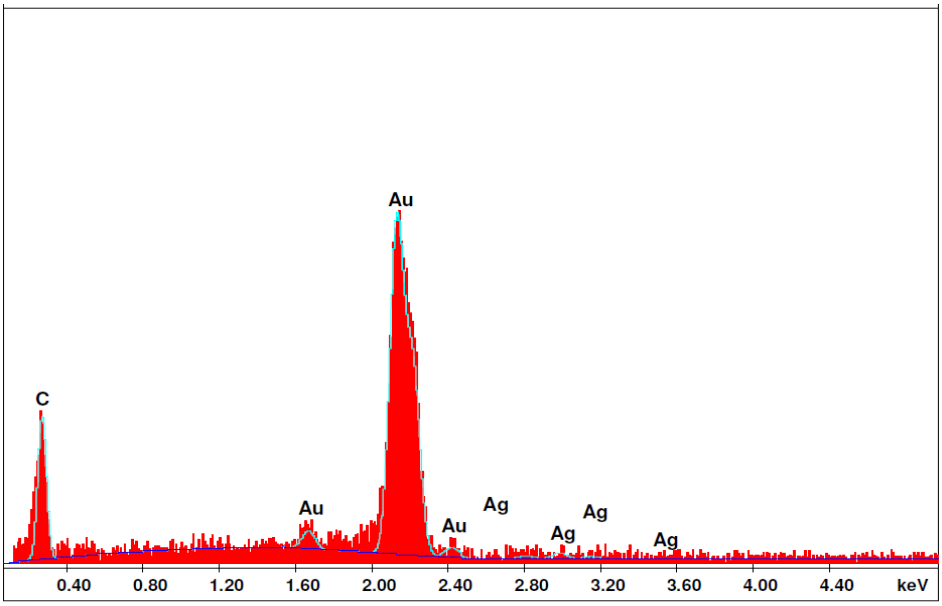

Fig. 36: EDS confirming the presence of Ag nanoparticles in 20 wt.% Ag/*f*N-CNTs/β-CD polymer nanocomposite.

5.2.4 Surface area of 20wt%Agf/N-CNTs/β-CD polymer nanocomposite

The surface area of the 20 wt.% Ag/*f*N-CNTs/β-CD polymer nanocomposite was found to be 1.2 m^2/g. The surface area of this composite is higher compared to similar materials synthesized *via* the conventional method in previous studies [116]. The microwave method does not only provide faster and efficient times as reported earlier but also allow for efficient structuring of the all three components of the composite for improved surface area.

5.3 Removal of bisphenol A, trichloroethylene and *p*-nitrophenol by Ag/*f*N-CNTs/ β-CD polymer nanocomposites

The synthesized Ag/*f*N-CNTs/ β-CD polymer nanocomposites displayed excellent absorption of bisphenol A, trichloroethylene and *p*-phenol, all prominent organic pollutants in water systems (Table 5). Similar results were obtained in earlier studies which used the conventional method to synthesize CD based polymers [3, 10, 15, 79, 112, 116-118]. These results suggest that microwave irradiation does not restructure or destroy the β-CD but they

remain intact to remove the organic pollutants. The ease with which the polymers could be synthesized using microwaves cannot be over emphasized. The polymers could be produced reproducibly and 16 batches of the polymers could be synthesized within 10 min.

Table 7: Amounts (percentage) of organic pollutant removed after passing water samples containing 20 µg/L of pollutant through the Ag/N-CNT/β-CD polymer nanocomposites

Pollutant	Absorbing Material Used:	
	Conventional – 24 h	**Microwave – 10 min.**
	Percentage Pollutant Removal	
Bisphenol A	93	100
Trichloroethylene	95	99
Para-nitrophenol	90	99

NB: Percentages are an average of 5 experiments.

The synthesized polymer nanocomposites have shown to maintain the same removal efficiency for over 5 cycles of percolating the media with 30 ml water samples. The regeneration of the materials once the removal efficiency drops is a simple process. It involves the use of a non-polar solvent such as ethanol. The non-polar media favours hydrophobic interactions with the phenols thus forcing them out from the cavity of the CD [79]. Once regenerated, the polymer is ready for use again.

5.4 Antibacterial studies

5.4.1 *Bacterial activity of 20 wt.% Ag/fN-CNTs*

Prior to testing the 20 wt.% Ag/*f*N-CNTs/β-CD polymer nanocomposites against *E. coli,* the 20 wt.% Ag/*f*N-CNTs were tested to confirm that Ag on the *f*N-CNTs can indeed destruct the bacteria before they can be embedded in the polymer matrix. After making the appropriate dilutions of the cultures, the standard concentration of *E. coli* was 1 x 10^5 cells/ml prior to treatment. Ag/N-CNTs were then placed in 10 ml of culture (for 24 h) and spotted on

HiChrome plates with standard concentration of cells. After a 24 h exposure to the polymer matrix, the number of *E. coli* cells was reduced to 4.7 x 10^3 cells/ml (a 95% reduction) and an inhibition zone of 3.2 cm was observed. This is a significant reduction; thus confirming the efficiency of the Ag/*f*N-CNTs material against the bacterial cell lysis. The images below show the plates before and after 24 h. The diameter of zone of inhibition can be noted in these images (Fig. 37).

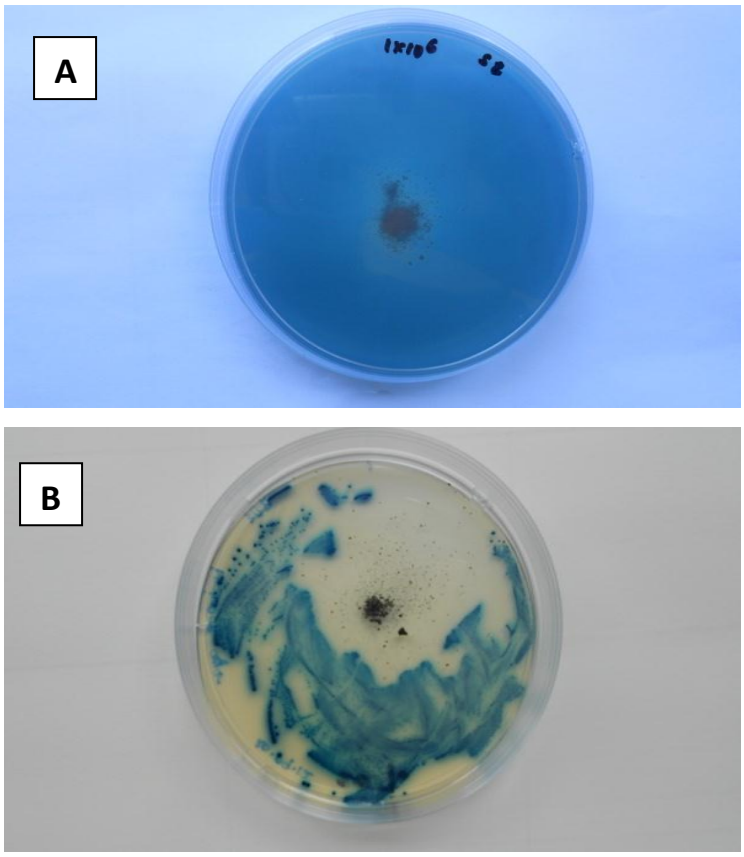

Fig. 37: Images showing the zone of inhibition at time 0 (a) and after 24 h (b)

5.4.2 *Bacterial activity of 20wt%Ag/fN-CNTs/*β-CD *polymer nanocomposite*

The 20 wt.% Ag/*f*N-CNTs/β-CD nanocomposite material was tested for its efficiency against the removal of *E. coli*. Table 6 shows the concentration of *E. coli* cells after 3 and 24 h of exposure to the polymer composite. The results indicate an increase in the amount of *E. coli* cells with time. There are a number of possible reasons attributed to this: Firstly, Ag nanoparticles within the polymer matrix might not be highly exposed to the bacterial cells but rather hidden within the polymer matrix thus making it hard for the antibacterial activity to be

efficient [119]. Secondly, agglomeration of N-CNTs due to van der waals forces makes it hard to disperse in polymer matrix [120]. The implications of this would be the entrapment of Ag nanoparticles within the folded N-CNTs thus reducing the amount of Ag accessible for bacterial degradation. In addition, the uptake of Ag nanoparticles by the bacterial cell membrane over time can significantly reduce the amount of Ag available for sustainable bacterial degradation [121]. Considering that 1% (w/w) of 20 wt.% Ag/*f*N-CNTs was polymerised with β-CD, with a 0.2% total of Ag available in the polymer composite, any uptake would quickly reduce the available amount of Ag and cause a decline in the efficiency of the system to degrade bacteria for a prolonged period.

Table 8: *E. coli* cell counts after 3 and 24 h of exposure to 20 wt.% Ag/N-CNTs/β-CD polymer nanocomposite. Concentration of cells at start: **3×10^5.**

Replicate	**Cells/ml after 3 h**	**Cells/ml after 24 h**
1	2.7×10^8	3.2×10^8
2	2.7×10^8	6.5×10^8
3	5.7×10^6	4.5×10^8

CHAPTER 6: CONCLUSIONS AND RECOMMENDATIONS

6.1 Conclusions

The project successfully achieved all the set objectives. The following conclusions were drawn from the study:

- The 10wt% Fe-Co/$CaCO_3$ catalyst was successfully synthesized using the wet impregnation method and it was found suitable to synthesize N-CNTs that contained a 2% N content. The reactivity of the N-CNTs was improved by modifying the surface with carboxyl groups during acid treatment. Zeta potential measurements and FT-IR analysis of the functionalized N-CNTs provided useful information on the type and degree of functionalization of the N-CNTs.

- The dispersion of Ag nanoparticles onto *f*N-CNTs was successfully achieved using a modified microwave irradiated polyol method. TEM analysis confirmed the synthesis of very small particles of Ag, with average diameters of 3.5 nm, which were required for bacterial destruction.

- *f*N-CNTs/β-CD and Ag/*f*N-CNTs/β-CD were successfully synthesized for the first time using microwave irradiation method. The method is cost-effective, greener and provides useful polymer nanocomposites within a period of 10 min as opposed to the conventional methods that can take up to 24 h.

- The TGA technique was used to confirm the stability of the polymer composites and it was observed that they were stable across a wide temperature range, 100-400 ^{o}C.

- Different parameters of the microwave method were explored. It could be concluded that 600 W power and 10 min were optimum parameters for the synthesis of the nanocomposites. The microwave produced very porous and less densely packed polymer nanocomposites with higher surface areas, a requirement for efficient pollutant absorption. It is worth noting however, that CD polymers generally have a very low surface area. Their mechanism of absorption of pollutants however supersedes the notion that a higher surface area always provides the best results. For this reason, the materials are suitable to remove pollutants present at very low concentrations.

- The microwave synthesized polymer composites were found to be efficient in the removal of prominent organic pollutants, bisphenol A, *p*-nitrophenol and trichloroethylene, in spiked water samples as indicated by UV-Vis and GC/MS. Further, antibacterial investigations demonstrate that the nanocomposites are capable of destroying *E. coli* species in water.

6.2 Recommendation for future work

Several recommendations that emanated from the findings of the project are described below:

- A study that will look into an optimum loading of Ag to ensure efficient bacterial destruction as a function of time is necessary to ensure optimum destruction of the bacteria in water samples.

- Testing the efficiency of the polymer nanocomposites against organics in real water systems must be carried out. At the time of submission of this thesis, samples from Rand Water Plant and Johannesburg Water, Northern Works, had been obtained to carry out this work. The data will be published.

- Studies on the health implication of these polymers on humans are necessary.

REFERENCES

1. Pradeep T, Anshup S (2009) *Thin Solid Films* **517**, 6441-6478

2. Li Q, Mahendra S, Lyon DY, Brunet L, Liga MV, Li D, Alvarez PJJ (2008) *Water Research* **42**, 4591-4602

3. Salipira KL, Krause RW, Mamba BB, Malefetse TJ, Cele LM, Durbach SH (2008) *Materials Chemistry and Physics* **111**, 218-224

4. Croft AP, Bartsch RA (1983) *Tetrahedron* 39, 1417-1474

5. Mahendra S, Li Q, Lyon DY, Brunet L, Alvarez PJJ (2009) William Andrew Publishing, Boston 157-166

6. Nagy NM, Kónya J, Beszeda M, Beszeda I, Kálmán E, Keresztes Z, Papp K, Cserny I (2003) *Journal of Colloid and Interface Science* **263**, 13-22

7. Kasprzyk-Hordern B (2004) *Advances in Colloid and Interface Science* **110**, 19-48

8. Xiao-qin Li, Wei-xian Zhang (2006) *Sciences* **31**, 111-122

9. Cafer T. Yavuz JTM, Yu WW, Prakash A, Falkner JC, Yean S, Cong L, Shipley HJ, Kan A, Tomson M, Natelson D, Colvin VL (2006) *science* **316**, 964-967

10. Salipira KL, Mamba BB, Krause RW, Malefetse TJ, Durbach SH (2007) *Environmental Chemistry Letters* **5**, 13-17

11. Shao L, Mu C, Du H, Czech Z, Du H, Bai Y (2011) *Applied Surface Science* **258**, 1682-1688

12. Shao D, Sheng G, Chen C, Wang X, Nagatsu M (2010) *Chemosphere* **79**, 679-685

13. Mamba G, Mubianda XY, Govender PP , Mamba BB, Krause RW (2010) *Journal of Applied Sciences* **10**, 940-949

14. Girek T, Shin DH, Lim ST (2000) *Carbohydrate Polymers* **42**, 59-63

15. Mhlanga SD, Mamba BB, Krause RW, Malefetse TJ (2007) *Journal of Chemical Technology & Biotechnology* **82**, 382-388

16. Nxumalo EN, Coville NJ (2010) *Review. Materials* **3**, 2141-2171

17. Ayala P, Arenal R, Rümmeli M, Rubio A, Pichler T (2010) *Carbon* **48**, 575-586

18. Motshekga S, Pillai SK, Ray SS, Jalama K, Krause RWM (2012) *Journal of Nanomaterials* **2012,** 1-15

19. Chen W, Zhao J, Lee JY, Liu Z (2005) *Materials Chemistry and Physics* **91**, 124-129

20. Mamba BB, Krause RW, Malefetse TJ, Mhlanga SD, Sithole SP, Salipira KL and Nxumalo EN (2007) *Water SA* **33**, 223-227

21. Matilainen A, Sillanpää M (2010) *Chemosphere* **80**, 351-365

22. Manojlovic D, Ostojic DR, Obradovic BM, Kuraica MM, Krsmanovic VD, Puric J (2007) *Desalination* **213,** 116-122

23. Chow CWK, Fabris R, Drikas M (2004) *Journal of Water Supply: Research and Technology* **53**, 85-92

24. Matilainen A, Vepsäläinen M, Sillanpää M (2010) *A review. Advances in Colloid and Interface Science* **159**, 189-197

25. Sarathy S, Mohseni M (2010) *Water Research* **44**, 4087-4096

26. Asan A, Isildak I (2003) *Journal of Chromatography* **988**, 145-149

27. Bigley FP, Grob RL (1985) *Journal of Chromatography* **350**, 407-416

28. Bhatti ZI, Toda H, Furukawa K (2002) *Water Research* **36**, 1135-1142

29. (1992): Agency for Toxic Substances and Disease Registry (ATSDR). Toxicological profile for nitrophenols: 2-nitrophenol and 4-nitrophenol. US Department of Health and Human Services, Public Health Service, Atlanta, USA, .

30. Heo J, Flora JRV, Her N, Park Y-G, Cho J, Son A, Yoon Y (2012) *Separation and Purification Technology* **90**, 39-52

31. Zhang Y, Causserand C, Aimar P, Cravedi JP (2006) *Water Research* **40**, 3793-3799

32. Liu W, Zhang H, Cao B, Lin K, Gan J (2011) *Water Research* **45**, 1872-1878

33. Watson RE, Jacobson CF, Williams AL, Howard WB, DeSesso JM (2006) *Reproductive Toxicology* **21**, 117-147

34. Steinberg AD, Desesso JM (1993) *Toxicology and Pharmacology* **18**, 137-153

35. Loeber CP, Hendrix MJC, De Pinos SD, Goldberg SJ (1988) *Pediatr Res* **24**, 740-744

36. Ates N, Kaplan SS, Sahinkaya E, Kitis M, Dilek FB, Yetis U (2007) *Journal of Hazardous Materials* **142**, 526-534

37. Nishijima W, Fahmi, Mukaidani T, Okada M (2003) *Water Research* **37**, 150-154

38. Muhammad S, Shah MT, Khan S (2011) *Microchemical Journal* **98**, 334-343

39. Chanpiwat P, Sthiannopkao S, Kim K-W (2010) *Microchemical Journal* **95**, 326-332

40. Muhammad S, Tahir SM, Khan S (2010) *Food and Chemical Toxicology* **48**, 2855-2864

41. Ritchie SMC, Bhattacharyya D (2002) *Journal of Hazardous Materials* **92**, 21-32

42. Lee Y-C, Park W-K, Yang J-W (2011) *Journal of Hazardous Materials* **190**, 652-658

43. Theis TL, Iyer R, Kaul LW (1988) *Environmental Science & Technology* **22**, 1013-1017

44. Hong H-j, Kim H, Baek K, Yang J-W (2008) *Desalination* **223**, 221-228

45. Ratnayaka DD, Brandt MJ, Johnson KM (2009) Butterworth-Heinemann, Boston, 195-266

46. Deng M, Lancto CA, Abrahamsen MS (2004) *International Journal for Parasitology* **34**, 73-82

47. Franzen C, Müller A (1999) *Diagnostic Microbiology and Infectious Disease* **34**, 245-262

48. An Y-J, Kampbell DH, Peter Breidenbach G (2002) *Environmental Pollution* **120,** 771-778

49. Avery LM, Williams AP, Killham K, Jones DL (2008) *Science of The Total Environment* **389**, 378-385

50. Fernandez MI, Sansonetti PJ (2003) *International Journal of Medical Microbiology* **293**, 55-67

51. Ge F, Zhu L, Chen H (2006) *Journal of Hazardous Materials* **133**, 99-105

52. Yang H, Cheng H (2007) *Separation and Purification Technology* **56**, 392-396

53. council wc (2008): drinking water chlorination.

54. Katherine H, Baker JPH, Redmond B, Reed NA, Herson DS (2002) *Appl. Environ. Microbiol.* **68**, 981-984

55. Lefebvre E, Racaud P, Parpaillon T, Deguin A (1995) *Science and Engineering* **17,** 311-327

56. von Gunten U, Hoigne J (1994) *Environmental Science & Technology* **28**, 1234-1242

57. Chevremont AC, Farnet AM, Coulomb B, Boudenne JL (2012) *Science of The Total Environment* **426**, 304-310

58. Lehtola MJ, Miettinen IT, Vartiainen T, Rantakokko P, Hirvonen A, Martikainen PJ (2003) *Water Research* **37**, 1064-1070

59. Liberti L, Notarnicola M, Petruzzelli D (2003) *Desalination* **152**, 315-324

60. Wang X, Hu X, Wang H, Hu C (2012) *Water Research* **46**, 1225-1232

61. Xing W, Ngo HH, Kim SH, Guo WS, Hagare P (2008) *Bioresource Technology* **99**, 8674-8678

62. Aktaş Ö, Çeçen F (2007) *Biodegradation* **59**, 257-272

63. Dhakras PA (2011) A review, Nanoscience, Engineering and Technology (ICONSET), 2011 International Conference on, 285-291

64. Loo S-L, Fane AG, Krantz WB, Lim T-T (2012) *Water Research* **46**, 3125-3151

65. Fane AG, Tang CY, Wang R (2011) *Water Science*, 301-335

66. Hsiue G-H, Pung L-S, Chu M-L, Shieh M-C (1989) *Desalination* **71**, 35-44

67. Holloway RW, Childress AE, Dennett KE, Cath TY (2007) *Water Research* **41**, 4005-4014

68. Bouguecha S, Hamrouni B, Dhahbi M (2005) *Desalination* **183**, 151-165

69. Susanto H (2011) *Process Intensification* **50**, 139-150

70. Klimkova S, Cernik M, Lacinova L, Filip J, Jancik D, Zboril R (2011) *Chemosphere* 82, 1178-1184

71. Kiliaris P, Papaspyrides CD (2010) *Progress in Polymer Science* **35**, 902-958

72. Giannelis EP (1996) *Advanced Materials* **8**, 29-35

73. Lan T, Pinnavaia TJ (1994) *Chemistry of Materials* **6**, 2216-2219

74. LeBaron PC, Wang Z, Pinnavaia TJ (1999) *Applied Clay Science* **15**, 11-29

75. Dash M, Chiellini F, Ottenbrite RM, Chiellini E (2011) *Progress in Polymer Science* **36**, 981-1014

76. Chandy T, Sharma CP (1990) *Artificial Cells, Blood Substitutes and Biotechnology* **18**, 1-24

77. Szejtli J (1998) *Chemical Reviews* **98**, 1743-1754

78. Vončina B, Vivod V, Jaušovec D (2007) *Dyes and Pigments* **74**, 642-646

79. Li D, Ma M (2000) *Clean Technologies and Environmental Policy* **2**, 112-116

80. Rekharsky MV, Inoue Y (1998) *Chemical Reviews* **98**, 1875-1918

81. Li D, Ma M (1999): *CHEMTECH* **29**, 31-37

82. Iijima S (1991) *Nature* 354, 56-58

83. Coleman JN, Khan U, Blau WJ, Gun'ko YK (2006) *Carbon* **44**, 1624-1652

84. Cui S, Canet R, Derre A, Couzi M, Delhaes P (2003) *Carbon* **41**, 797-809

85. Baughman RH, Zakhidov AA, de Heer WA (2002) *Science* **297**, 787-792

86. Lafuente E, Callejas MA, Sainz R, Benito AM, Maser WK, Sanjuán ML, Saurel D, de Teresa JM, Martínez MT (2008) *Carbon* **46**, 1909-1917

87. Coville NJ, Mhlanga SD, Nxumalo EN, Shaikjee A (2011) *South African Journal of Science* **107**, 01-15

88. Matus KJM, Xiao X, Zimmerman JB (2012) *Journal of Cleaner Production* **32**, 193-203

89. Anastas PT, Zimmerman JB (2003) *Environmental Science & Technology* **37**, 94A-101A

90. Bilecka I, Niederberger M (2010) *Nanoscale* **2**, 1358-1374

91. Hoogenboom R, Wilms TFA, Erdmenger T, Schubert US (2009) *Australian Journal of Chemistry* **62**, 236-243

92. Kappe CO (2004) *Angewandte Chemie International Edition* **43**, 6250-6284

93. Bilecka I, Hintennach A, Djerdj I, Novak P, Niederberger M (2009) *Journal of Materials Chemistry* **19**, 5125-5128

94. Menéndez JA, Arenillas A, Fidalgo B, Fernández Y, Zubizarreta L, Calvo EG, Bermúdez JM (2010) *Fuel Processing Technology* **91**, 1-8

95. Berlan J (1995) *Radiation Physics and Chemistry* **45**, 581-589

96. Tsai C-C, Rubin B, Tatartschuk E, Owens J R, Luzinov I and Kornev K G (2012) *Journal of Engineered Fibers and Fabrics* **7**, 42-49

97. Antonetti C, Oubenali M, Raspolli Galletti AM, Serp P, Vannucci G (2012) *Applied Catalysis A: General* **421–422**, 99-107

98. Sosnik A, Gotelli G, Abraham GA (2011) *Progress in Polymer Science* **36**, 1050-1078

99. Mhlanga SD, Mondal KC, Carter R, Witcomb MJ, Coville NJ (2009) *South African Journal of Chemistry* **62**, 67-76

100. Tetana ZN, Mhlanga SD, Bepete G, Krause RWM, Coville NJ (2012) *South African Journal of Chemistry* **65**, 39-49

101. Magrez A, Seo J W, Smajda R, Mionic M, Forro L (2010) *Materials* **3**, 4871-4891

102. See CH, Harris AT (2008) *AIChE Journal* **54**, 657-664

103. Bahome MC, Jewell LL, Hildebrandt D, Glasser D, Coville NJ (2005) *Applied Catalysis A: General* **287**, 60-67

104. Biddinger E.J, von Deak D, Ozkan U.S. (2009) *Catal.* **52,** 1566

105. van Dammele S, Romero-Izquirdo A., Brydson R., de Jong K.P., J.H B (2008) *Carbon* **46**, 138

106. Li Q, Yan H, Zhang , Liu J (2004) *Carbon* **42**, 829

107. Kang Z C, Wang Z L (1996): *J. Phys. Chem*. **100**, 5163

108. Wang Z. L., Kang Z. C. (1996): J. Phys. Chem. 100, 17725

109. Motchelaho MAM, Xiong H, Moyo M, Jewell LL, Coville NJ (2011) *Journal of Molecular Catalysis A: Chemica*l **335**, 189-198

110. Moreno-Castilla C, Ferro-Garcia MA, Joly JP, Bautista-Toledo I, Carrasco-Marin F, Rivera-Utrilla J (1995 *Langmuir* **11**, 4386-4392

111. Yu X, Lin B, Gong B, Lin J, Wang R, Wei K (2008) *Catal Lett* **124,** 168-173

112. Li D, Ma M (1999) *Filtration & Separation* **36**, 26-28

113. Gerbec JA, Magana D, Washington A, Strouse GF (2005) *Journal of the American Chemical Society* **127**, 15791-15800

114. Tsai C, Rubin B, Tatartschuk E, Owens JR, Luzinov I, KG K (2012) *Journal of Engineered Fibers and Fabrics* **7**, 42-49

115. Mhlanga SD, Masinga SP, Bambo MF, Mamba BB, Nxumalo EN (2013) *Nanoscience and Nanotechnology letters* **5**, 1-8

116. Lukhele LP, Krause RWM, Mamba BB, Momba MNB (2010) *Water SA* **36**, 433-436

117. Mamba B, Krause R, Malefetse T, Gericke G, Sithole S (2008) *Water SA* **34,** 657-660

118. Mamba G, Mbianda XY, Govender PP, Krause RW (2010) *Journal of Applied Sciences* **10**, 940-949

119. Dallas P, Sharma VK, Zboril R (2011) *Advances in Colloid and Interface Science* **166**, 119-135

120. Sahoo NG, Rana S, Cho JW, Li L, Chan SH (2010) *Progress in Polymer Science* **35**, 837-867

121. Gupta P, Bajpai M, Bajpai SK (2008) *Journal of Cotton Science* **12**, 280-286